Encyclopedia of Paleoclimatology and Ancient Environments

2009 Edition
Lonnie G. Thompson
Reference work entry
DOI: https://doi.org/10.1007/978-1-4020-4411-3_111

ICE CORES, ANTARCTICA AND GREENLAND

Introduction

Polar ice results from the progressive densification of snow deposited at the surface of the ice sheet. The transformation of snow into ice generally occurs within the first 100 meters and takes from decades to millennia, depending on temperature and accumulation rate, to be completed. During the first stage of densification, recrystallization of the snow grains occurs until the closest dense packing stage is reached at relative densities of about 0.55–0.6, corresponding to the snow-firn transition. Then plastic deformation becomes the dominant process and the pores progressively become isolated from the surface atmosphere. The end product of this huge natural sintering experiment is ice, an airtight material. Because of the extreme climatic conditions, the polar ice is generally kept at negative temperatures well below the freezing point, a marked difference to the ice of temperate mountain glaciers.

Ice cores are cylinders of ice with a diameter of ~10 cm. They are obtained by drilling through glaciers or ice sheets. This entry deals with ice cores recovered in the two ice sheets existing today at the surface of the Earth: in Antarctica and Greenland. Ice cores from mountain glaciers are handled in another section (see *Ice cores, mountain glaciers*). Ice cores range from shallow (from the surface to 100 m), to intermediate (down to about 1,000 m) and deep (>1,000 m), and are recovered using specific technologies, including thermal and electromechanical drilling systems. The main purposes of recovering ice cores in Antarctica or Greenland are to describe the past changes in atmospheric composition and climate of our planet, understand the past behavior of the ice sheets and the mechanisms controlling ice flow, and ultimately contribute to an improved understanding of the Earth system.

The main Antarctic and Greenland ice cores

Apart from several shallow drilling sites in the most coastal area and a few drillings through the ice shelves, a total of 14 drill cores have reached bedrock or a depth close to bedrock in Antarctica and Greenland. Therefore, the current number of drill sites is still fairly limited in relation to the large dimensions of these ice sheets. Table I1 provides information on the ten deepest drilling operations; Figures I1 and I2 show their location in Antarctica and Greenland.

Two pioneering long ice cores, the Camp Century (Greenland) (Hansen and Langway Jr., 1966; Dansgaard et al., 1971) and the Byrd (West Antarctica) (Gow et al., 1968; Epstein et al., 1970) cores, drilled in the 1960s, provided the first continuous and already detailed record back to the last deglaciation and the last ice age.

Three deep Antarctic ice cores record several glacial-interglacial cycles: Vostok (4 cycles, back to 420 kyBP; Petit et al., 1999), Dome Fuji (DF) (3 cycles, 330 kyBP; Watanabe et al., 2003) and EPICA Dome C (EDC) (8 cycles, 740 kyBP; EPICA Community Members, 2004, Figure I3).

The Vostok drill site holds the world's record in terms of depth, as of 2007. The EDC core, although shorter by a few hundred meters, provides the longest record, approximately twice as old as the Vostok record. New measurements are performed to extend the EDC record back to 800,000 yBP. Furthermore, a new deep drilling at DF, completed in 2006, lies close to bedrock. It should provide the second longest record, covering ~700,000 years.

Three long Greenland ice cores, GRIP, GISP2 and NGRIP cover the last 100,000 years; i.e., most of the last glacial-interglacial cycle, but only the NGRIP core provides an undisturbed record back to the latest part of the penultimate interglacial (also called Eemian) (North Greenland Ice Core Project Members, 2004). A new drilling operation (called NEEM) is planned in Greenland to recover an ice core able to provide a complete record of the Eemian. In addition, a number of intermediate-type cores recovered from both ice sheets sample the Holocene (our current interglacial) and part of the last glacial period with good resolution.

Establishing an ice core chronology

Establishing the chronology of Antarctic and Greenland ice cores is essential for interpreting ice core records. The age of the ice corresponds to the time the snow is deposited at

Table I1 Major ice cores: sites, depth, length of record. Please, note that in most cases, we use the first publication that provides the basic information, rather than the most recent or most relevant ones

Site	Ice sheet	Year of recovery	Depth (m)	Temporal length of the record
Camp Century (Dansgaard et al., 1971)	Greenland	1966	1,387.4	Back to the last ice age
Byrd (Epstein et al., 1970; Gow et al., 1968)	West Antarctica	1968	2,164	Back to the last ice age
Dye 3 (Dansgaard et al., 1985)	Greenland	1981	2,037	Back to the last ice age
GRIP (GREENLAND-SUMMIT-ICE-CORES, 1997)	Greenland	1992	3,029	~105 ka
GISP 2 (GREENLAND-SUMMIT-ICE-CORES, 1997)	Greenland	1993	3,053	~105 ka
Vostok (Petit et al., 1999)	East Antarctica	1998	3,623	~420 ka
North GRIP (NORTH-GREENLAND-ICE-CORE-PROJECT-MEMBERS, 2004)	Greenland	2003	3,085	~120 ka
EPICA DC (EPICA-COMMUNITY-MEMBERS, 2004)	East Antarctica	2004	3,270	~800 ka
EPICA DML (EPICA-COMMUNITY-MEMBERS, 2006)	East Antarctica	2006	2,774	More than one glacial-interglacial cycle
Dome Fuji	East Antarctica	2006	3,029	The age at the bottom is estimated to be ~700 ka

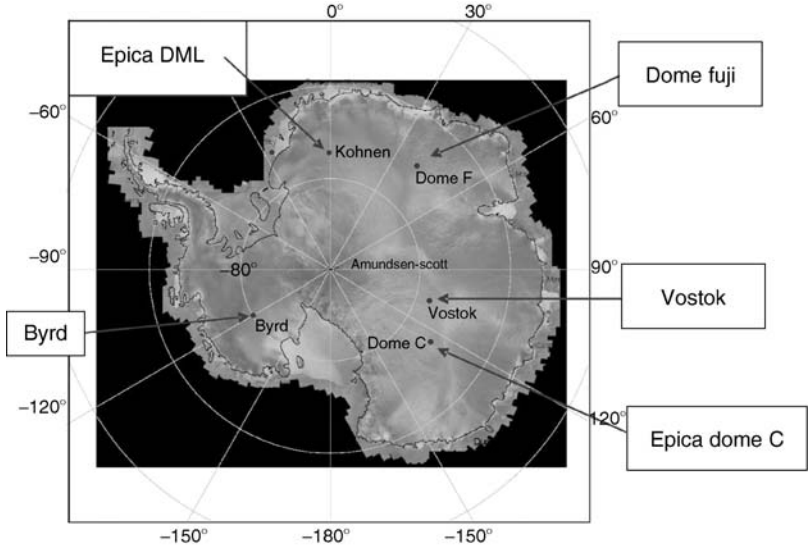

Figure I1 Index map showing the locations of ice cores from Antarctica that are listed in Table I1.

the surface of the ice sheet and its chronology can be established using different tools including layer counting, synchronization to the Earth orbital variations (orbital tuning approach), synchronization to other well dated archives, and glaciological modeling. On the other hand, during snow densification, interstitial air can exchange with the atmosphere at the surface through the firn porosity until it is trapped in the form of bubbles. Therefore, in any ice core, contemporaneous gas and ice signals are not recorded at the same depth and air occluded in air bubbles is younger than its surrounding ice.

Note that methods based on radioactive decay are not of use to date polar ice directly. In particular, ^{14}C dating of the CO_2 trapped in air bubbles is possible but limited in accuracy because of in situ production in the firn.

Counting preserved annual layers through the seasonal variations of different properties, like ice isotopic composition, aerosol chemical composition or dust content, works in sites with high accumulation rates and is especially appropriate for Greenland ice cores. For instance, the method has been used on the DYE-3, GRIP, GISP2 and NGRIP cores, and can be especially accurate for Holocene ice (maximum counting error estimated to be up to 2%; Rasmussen et al., 2006). This layer counting method is, however, not applicable for low accumulation sites such as those of the East Antarctic Plateau. Orbital variations of the Earth impact the solar radiation received at the top of the atmosphere (generally called insolation), and in turn the Earth's climate. The orbital tuning approach consists of tuning ice core climatic records to those changes in insolation that can be accurately calculated for the past millions of years (Berger, 1978; Laskar et al., 2004). This approach has been used in the case of the long, 420-kyr Vostok record. Unfortunately, the phasing between insolation and the climatic response is generally poorly constrained and not likely to be constant due to the non-linearity of the climatic system, which is a major limitation of the orbital tuning approach. As a consequence, the chronological uncertainty of the orbital tuning approaches is about 5 kyr. Nevertheless, it has been recently suggested that ice core properties recording local insolation directly may overcome this limitation (Bender, 2002; Raynaud et al., 2007).

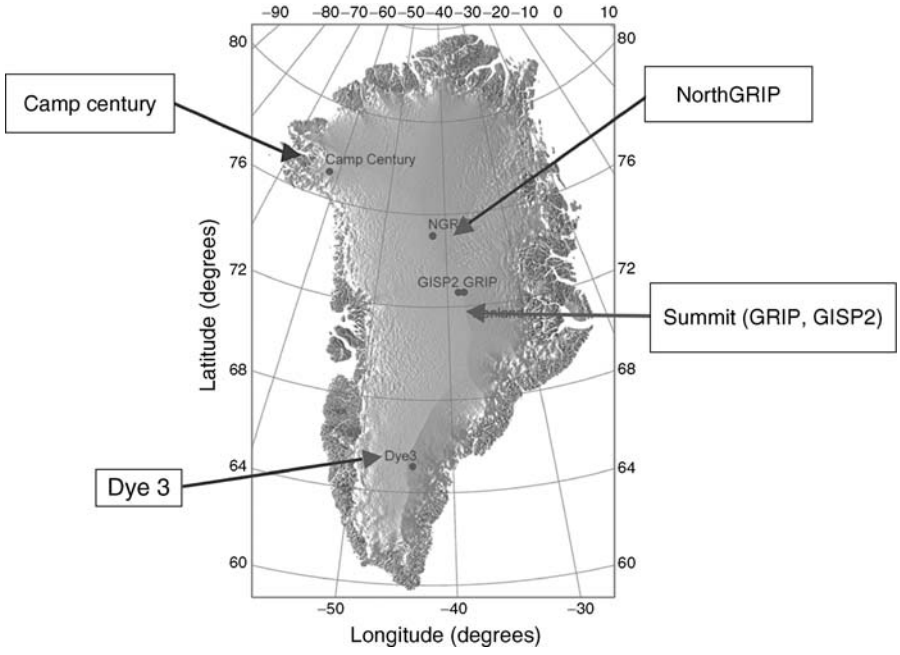

Figure I2 Index map showing the locations of ice cores from Greenland that are listed in Table I1.

Figure I3 Ice core protruding from the drill head from EPICA Dome C, Antarctica (photo courtesy of Eric LeFèbre, LGGE, Grenoble).

Ice cores can also be dated by synchronization with other well-dated archives. For example, back to the last glacial period, ice cores from Antarctica can be synchronized with the Greenland ice cores using the CH_4 records or the Be-10 records (Yiou et al., 1997; Blunier and Brook, 2001). A second example is the identification of well-dated volcanic eruptions in the ice cores.

In order to provide a method independent of the orbital tuning approach, glaciologists have proposed to date ice cores continuously using snow accumulation and ice flow models for calculating the annual layer thickness at each depth. In this case the main limitations include the uncertainties in our knowledge of past accumulation changes, basal conditions (melting, sliding) and rheological conditions.

Finally, it has been recently proposed to use an inverse method, which associates the information of the different dating methods available on one core to obtain an optimal chronology. This inverse method has been applied on the Vostok (Parrenin et al., 2001; Parrenin et al., 2004), Dome Fuji (Watanabe et al., 2003) and EPICA Dome C (EPICA Community Members, 2004) cores. In the future, such an inverse method could be applied to several drilling sites simultaneously, obtaining a common and optimal chronology for those drilling sites.

The difference between the ages of gas bubbles and the surrounding ice can be computed with a firn model (see Goujon et al., 2003 and references therein). Under present-day conditions, this difference is on the order of a few centuries for high accumulation/high temperature sites and of several thousands of years in sites of the high Antarctic Plateau with low accumulation and temperature conditions (e.g., ~3,000 years at Vostok). Under glacial conditions it increases significantly due to colder climate, which is paralleled by lower accumulation rates, but the accuracy of the calculation under past conditions is limited due to uncertainty in past accumulation rates and temperatures.

Antarctic and Greenland ice core: an archive of the atmospheric composition and climate

The Antarctic and Greenland ice cores contain a wide spectrum of information on past changes in the environmental conditions of the Earth. Examples are given in Table I2.

Polar ice cores record both variations in climate and in atmospheric composition. They essentially provide a pure record of solid precipitation, atmospheric gases, dust and aerosols and are, in fact, a unique archive of past changes of our atmosphere. For their part, deep oceanic and continental sediments are recording oceanic, vegetation or soil changes.

Table I2 Climatic or environmental parameters and corresponding properties measured in ice. Note the diversity of the information contained in ice cores, which deals with the atmosphere, the cryosphere, the oceans and the continents

Climatic and environmental parameter	Ice properties
Temperature change at the surface of the ice sheet	Isotopic composition of the ice ($^{18}O/^{16}O$, D/H); Isotopic composition of the air trapped in ice (^{15}N, ^{40}Ar)
Variations of atmospheric greenhouse trace gases	Greenhouse trace gas concentrations in the air trapped in ice (CO_2, CH_4, N_2O)
Origin of the precipitation	Deuterium excess of ice
Atmospheric transport and circulation; Source (marine, continental, volcanic, anthropogenic) of dust and aerosols	Dust and aerosols in ice
Changes in continental ice volume and sea level; Changes in hydrological cycle and biological activity	Isotopic composition ($^{18}O/^{16}O$) of the atmospheric oxygen trapped in ice
Local insolation changes due to orbital cycles	O2/N2 of air trapped in ice; Air content of ice
Changes in surface elevation of the ice sheet	Air content of ice; Isotopic composition of ice
Changes in ice flow	Physical properties of ice
Solar activity and Earth's magnetic field intensity	Beryllium-10 (^{10}Be)

Continuous changes in temperature at the surface of the ice sheet are revealed by measuring the isotopic composition of the ice (deuterium or oxygen-18), and more sporadic abrupt temperature changes are accurately recorded by the isotopic composition of N_2 and Ar found in the air trapped in ice.

Polar ice cores also provide the most reliable paleo-archive of air composition, by directly recording atmospheric composition in the form of air bubbles when the firn becomes ice. They allow the reconstruction of the past evolution of important greenhouse gases (see section on carbon dioxide and methane, Quaternary variations). Thus, the Vostok and the new EPICA DC record produce clear evidence of the strong correlation between greenhouse gases (CO_2 and CH_4) and climate over glacial-interglacial cycles (EPICA Community Members, 2006; see also *Carbon dioxide and methane, Quaternary variations*).

Dust and aerosols found in Antarctic or Greenland ice cores have been collected at the surface of the ice sheets by dry or wet deposition. The ice record of their concentration and size distribution provides information about past extent of marine and continental sources as well as variations in atmospheric transport. Since marine sources can be influenced by the extent of sea ice, it may also be able to reconstruct past changes in sea ice. Ice cores also provide a precious volcanic record in the same way.

Apart from these natural variations in gases, dust and aerosols, ice cores record the impact of human activities, especially on greenhouse trace gases and sulfate compounds. They also document paleometallurgy activities from as early as Greek and Roman times and, during the last few decades, radioactive fallout and added lead in gasoline.

The ice core record also contains information about past changes of the ice sheets. The air content of polar ice depends on the atmospheric pressure when bubbles close-off, and thus gives information about past surface elevation. Physical properties of ice such as grain size and orientation are indicators of past ice flow in the vicinity of the drilling site.

Conclusion

Polar ice cores provide a wide range of information on the Earth system, some of which have a real impact on societal and educational issues. Because they play a central role in global change research, the international ice coring community is planning new projects in both Antarctica and Greenland under the International Partnerships in Ice Core Sciences (IPICS) initiative (Brook and Wolff, 2006). IPICS aims to extend the ice core record in time and enhance spatial resolution. Concerning deep ice coring, one of the projects is to search for a 1.5 million year record of climate and greenhouse gases in Antarctica, during a time period when Earth's climate shifted from ~40,000 year to ~100,000 year cycles. In northwest Greenland, a deep ice core is planned to recover a complete record of the Eemian for the first time.

Dominique Raynaud and Frédéric Parrenin

Bibliography

Bender, M., 2002. Orbital tuning chronology for the Vostok climate record supported by trapped gas composition. *Earth Planetary Sci. Lett.*, **204**, 275–289.

Berger, A.L., 1978. Long-term variations of daily insolation and Quaternary climatic changes. *J. Atmos. Sci.*, **35**, 2362–2367.

Blunier, T., and Brook, E.J., 2001. Timing of millennial-scale climate change in Antarctica and Greenland during the last glacial period. *Science*, **291**, 109–112.

Brook, E., and Wolff, E.W., 2006. The future of ice core science. *Eos Trans. AGU*, **87**(4), 39.

Dansgaard, W., Johnsen, S.J., Clausen, H.B., and Langway Jr., C.C. 1971. Climatic record revealed by the camp century ice core. In Turekian, K.K. (ed.), *The Late Cenozoic Glacial Ages.* New Haven, London: Yale University Press, pp. 37–56.

Dansgaard, W., Clausen, H.B., Gundestrup, N., Johnsen, S.J., and Rygner, C., 1985. Dating and climatic interpretation of two deep Greenland ice cores. In Langway Jr., C.C., Oeschger, H., and Dansgaard, W. (eds.), *Greenland Ice Core: Geophysics, Geochemistry and the Environment.* Washington, DC: Geophysical Monograph. American Geophysical Union.

EPICA Community Members, 2004. Eight glacial cycles from an Antarctic ice core. *Nature*, **429**(6992), 623–628.

EPICA Community Members, 2006. One-to-one coupling of glacial climate variability in Greenland and Antarctica. *Nature* **444**(7116), 195–198.

Epstein, S., Sharp, R.P., and Gow, A.J., 1970. Antarctic ice sheet: stable isotope analyses of Byrd station cores and interhemispheric climatic implications. *Science* **168**, 1570–1572.

Goujon, C., Barnola, J.-M., and Ritz, C., 2003. Modeling the densification of polar firn including heat diffusion: Application to close-off characteristics and gas isotopic fractionation for Antarctica and Greenland sites. *J. Geophys. Res.*, **108**. doi:10.1029/2002JD003319.

Gow, A.J., Ueda, H.T., and Garfield, D.E., 1968. Antarctic ice sheet: Preliminary results of first core hole to bedrock. *Science* **161**, 1011–1013.

Greenland Summit Ice Cores, 1997. *J. Geophys. Res.*, **102**(C12), 26315–26886.

Hansen, B.L., and Langway Jr., C.C., 1966. Deep core drilling in ice and core analysis at camp century, Greenland, 1961–1966. *Antarctic J. US*, **1**, 207–208.

Laskar, J., Robutel, P., Joutel, F., Gastineau, M., Correira, A.C.M., and Levrard, B., 2004. A long-term numerical solution for the insolation quantities of the Earth. *Astron Astrophys* **428**, 261–285.
North Greenland Ice Core Project Members, 2004. High-resolution record of Northern hemisphere climate extending into the last interglacial period. *Nature*, **431**, 147–151.
Parrenin, F., Jouzel, J., Waelbroeck, C., Ritz, C., and Barnola, J.-M., 2001. Dating the Vostok ice core by an inverse method. *J. Geophys. Res.*, **106** (D23), 31837–31851.
Parrenin, F., Rémy, F., Ritz, C., Siegert, M.J., and Jouzel, J., 2004. New modeling of the Vostok ice flow line and implication for the glaciological chronology of the Vostok ice core. *J. Geophys. Res.*, **109**. doi:10.1029/2004JD004561.
Petit, J.R., Jouzel, J., Raynaud, D., Barkov, N.I., Barnola, J.-M., Basile, I., Bender, M., Chappellaz, J., Davis, M., Delaygue, G., Delmotte, M., Kotlyakov, V.M., Legrand, M., Lipenkov, V.Y., Lorius, C., Pépin, L., Ritz, C., Saltzman, E., and Stievenard, M., 1999. Climate and atmospheric history of the past 420,000 years from the Vostok ice core, Antarctica. *Nature*, **399**, 429–436.
Rasmussen, S.O., Andersen, K.K., Svensson, A.M., Steffensen, J.P., Vinther, B.M., Clausen, H.B., Siggaard-Andersen, M.-L., Johnsen, S. J., Larsen, L.B., Dahl-Jensen, D., Bigler, M., Rothlisberger, R., Fischer, H., Goto-Azuma, K., Hansson, M.E., and Ruth, U., 2006. A new Greenland ice core chronology for the last glacial termination. *J. Geophys. Res.*, **111**, D06102. doi:10.1029/2005JD006079.
Raynaud, D., Lipenkov, V., Lemieux-Dudon, B., Loutre, M-F., Lhomme, N., 2007. The local insolation signature of air content in Antarctic ice: A new step toward an absolute dating of ice records. *Earth and Planetory Science Letters*, **261**, 337–349.
Watanabe, O., Jouzel, J., Johnsen, S., Parrenin, F., Shoji, H., and Yoshida, N., 2003. Homogeneous climate variability across East Antarctica over the past three glacial cycles. *Nature*, **422**, 509–512.
Yiou, F., Raisbeck, G.M., Baumgartner, S., Beer, J., Hammer, C., Johnsen, J., Jouzel, J., Kubik, P.W., Lestringuez, J., Stievenard, M., Suter, M., and Yiou, P., 1997. Beryllium 10 in the Greenland ice core project ice core at summit, Greenland. *J. Geophys. Res.*, **102**, 26783–26794.

Cross-references

Beryllium-10
Carbon Dioxide and Methane, Quaternary Variations
Deuterium, Deuterium Excess
Dust Transport, Quaternary
Ice Cores, Mountain Glaciers
Oxygen Isotopes
Quaternary Climate Transitions and Cycles
SPECMAP

ICE CORES, MOUNTAIN GLACIERS

Introduction

With the help of recent innovations in light-weight drilling technology, ice core paleoclimatic research has been expanded from the polar regions to ice fields in many of the world's mountain ranges and on some of the world's highest mountains. Over the last few decades, much effort has been focused on the retrieval of cores from sub-polar regions such as western Canada and eastern Alaska, the mid-latitudes such as the Rocky Mountains and the Alps, and tropical mountains in Africa, South America, and China. Unlike polar ice cores, climate records from lower-latitude alpine glaciers and ice caps present information necessary to study processes where human activities are concentrated, especially in the tropics and subtropics where 70% of the world's population lives. During the last 100 years, there has been an unprecedented acceleration in global and regional-scale climatic and environmental changes affecting humanity. The following is an overview of alpine glacier archives of past changes on millennial to decadal time scales. Also included is a review of the recent, global-scale retreat of these alpine glaciers under present climate conditions, and a discussion of the significance of this retreat with respect to the longer-term perspective, which can only be provided by the ice core paleoclimate records.

Locations of mountain ice core retrieval

The sites from which many of the high-altitude ice cores have been retrieved are shown in Table I3. Among the earliest efforts to retrieve climate records from mountain glaciers were programs involving surface sampling on the Quelccaya Ice Cap (13°56′ S, 70°50′ W; 5,670 m a.s.l.) in southern Peru (1974–1979). The results from this preliminary research, conducted by the Institute of Polar Studies (now the Byrd Polar Research Center) at The Ohio State University, paved the way for the first high-altitude tropical deep-drilling program on Quelccaya in 1983, which yielded a 1,500-year climate record. Meanwhile, in western Canada, a 103-m ice core was drilled on Mt. Logan (60°35′ N, 140°35′ W; 5,340 m a.s.l.) by Canada's National Hydrology Research Laboratory. The record from this core extends back to 1736 AD. Recently, the ice caps on both these mountains have been redrilled, Mt. Logan in 2002 and Quelccaya in 2003. During the intervening decades, mountain ice core research has expanded significantly throughout the world, with programs successfully completed on the Tibetan Plateau and the Himalayas, the Cordillera Blanca of Northern Peru, Bolivia, East Africa, the Swiss and Italian Alps, Alaska, and the Northwest United States (Table I3).

Climatic and environmental information from mountain ice cores

The records contained within the Earth's alpine ice caps and glaciers provide a wealth of data that contribute to a spectrum of critical scientific questions. These range from the reconstruction of high-resolution climate histories to help explore the oscillatory nature of the climate system, to the timing, duration, and severity of abrupt climate events, and the relative magnitude of twentieth century global climate change and its impact on the cryosphere. Much of the variety of measurements made on polar ice cores, and the resulting information, is also relevant to cores from mountain glaciers. Researchers can utilize an ever-expanding ice core database of multiple proxy information (i.e., stable isotopes, insoluble dust, major and minor ion chemistry, precipitation reconstruction) that spans the globe in spatial coverage and is of the highest possible temporal resolution. The parameters that can be measured in an ice core are numerous and can yield information on regional histories of variations in temperature, precipitation, moisture source, aridity, vegetation changes, volcanic activity and anthropogenic input (Figure I4). Many of these physical and chemical constituents produce wet and dry/cold and warm seasonal signals in the ice, which allow the years to be counted back similar to the counting of tree rings.

Isotopic ratios of oxygen and hydrogen (δ^{18}O and δD, respectively) are among the most widespread and important of the measurements made on ice cores. Early work on polar ice cores on these "stable" (i.e., as opposed to unstable, or radioactive) isotopes indicated that they provide information on the precipitation temperature (Dansgaard, 1961), based on

Table I3 A sampling of mountain glaciers sites from which ice cores have been retrieved since 1980. This is by no means a complete inventory of all alpine ice cores ever collected

Mountain	Location	Elevation (m a.s.l.)	Year drilled	Leading organization	Length of core (m)	Length of record (yr)
Bona Churchill	61°24′ N, 141°42′ W	4,420	2002	BPRC	460	1700
Mt. Logan	60°35′ N, 140°35′ W	5,340	1980	NHRI	103	225
			2002	NGP, AINA	190	NA
				NIPR	220	NA
				IQCS, UNH	345	NA
Eclipse Dome	60°51′ N, 139°47′ W	3,017	1996	UNH	160	NA
Fremont Glacier	49°07′ N, 109°37′ W	4,100	1991	USGS	160	275,
			1998		50, 160	NA
Belukha	49°48′ N, 86°34′ E	4,062	2001	PSI, UNIBE	140	200+
Fiescherhorn	46°32′ N, 8°02′ E	3,880	1988	PSI, UNIBE	30	42
			2002		150	
Coropuna	15°32′ S, 72°39′ W	6,450	2003	BPRC	146.3, 34.3, 34.3	16,000+
Col du Dôme	45°50′ N, 6°50′ E	4,250	1994	LGGE, IFU	139	75
Mont Blanc	45°45′ N, 6°50′ E	4,807	1994	LGGE	140	200+
Djantugan	43°12′ N, 42°46′ E	3,600	1983	IGRAS	93	57
Gregoriev	41°58′ N, 77°55′ E	4,660	1991	IGRAS, BPRC	20, 16	53
			2001	IGRAS	21.5	NA
			2003	IGRAS	22	NA
Dunde	38°06′ N, 96°24′ E	5,325	1987	BPRC, LIICRE	138	10,000+
Malan	35°50′ N, 90°40′ E	6,056	1999	LIICRE	102	112+
Guliya	35°17′ N, 81°29′ E	6,200	1992	BPRC, LIICRE	302	110,000+
Puruogangri	33°55′ N, 89°05′ E	6,000	2000	BPRC, LIICRE	208	7000
Dasuopu	28°23′ N, 85°43′ E	7,200	1996	BPRC, LIICRE	162	1,000+
Qomolangma	27°59′ N, 86°55′ E	6,500	1998	UNH, LIICRE	80	154
Kilimanjaro	3°04′ S, 37°21′ E	5,895	2000	BPRC	52	11,700
Huascarán	9°06′ S, 77°36′ W	6,050	1993	BPRC	166	19,000
Quelccaya	13°56′ S, 70°50′ W	5,670	1983	BPRC	155, 164	1,500
			2003		168, 129	1780
Illimani	16°37′ S, 67°47′ W	6,350	1999	IRD, PSI	137, 139	18,000
Sajama	18°06′ S, 68°53′ W	6,540	1996	BPRC	132	20,000

NA: Data not available.
Abbreviations: *BPRC*, Byrd Polar Research Center, The Ohio State University (USA); *NHRI*, National Hydrology Research Institute (Canada); *NGP*, National Glaciology Program (Canada); *AINA*, Arctic Institute of North America, University of Calgary (Canada); *NIPR*, National Institute of Polar Research (Japan); *IQCS*, Institute for Quaternary and Climate Studies, University of Maine (USA); *USGS*, United States Geological Survey (USA); *PSI*, Paul Scherrer Institute (Switzerland); *IRD*, Institute of Research and Development (France); *LGGE*, Laboratoire de Glaciologie et Geophysique de l'Environnement (France); *IGRAS*, Institute of Geography, Russan Academy of Science (Russia); *IFU*, Institut für Umweltphysik (Germany); *UNIBE*, University of Bern (Switzerland); *LIICRE*, Key Laboratory of Ice Core and Cold Regions Environment (China); *UNH*, Institute for the Study of Earth, Oceans and Space, University of New Hampshire (USA).

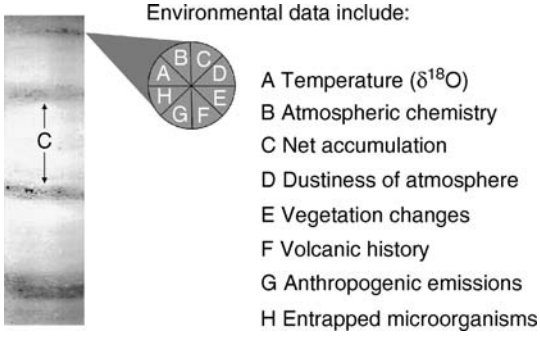

Figure I4 A large variety of environmental information can be obtained from high-altitude ice cores. On the *left* is an image of a core from a typical mountain glacier in Tibet. The dust bands were deposited during the dry seasons, and the space between them is cleaner ice from snow deposited during the wet seasons.

the fractionation of the oxygen and hydrogen atoms into their light and heavy isotopes (^{16}O and ^{18}O, ^{1}H and ^{2}H or deuterium (D)), and on the higher vapor pressure of $H_2{}^{16}O$ over $HD^{16}O$ and $H_2{}^{18}O$. The resulting ratios of the light and heavy isotopes of these elements act as recorders of temperature both at the moisture source and at the deposition site.

The use of $\delta^{18}O$ and δD as temperature proxies for polar ice is now widely accepted; however, it is still a source of controversy for lower-latitude cores. Some who have studied the problem suggest that $\delta^{18}O$, rather than being a temperature recorder at lower latitudes, is a function of precipitation amount (Rozanski et al., 1993; Dahe et al., 2000; Shichang et al., 2000; Baker et al., 2001; Tian et al., 2001). However, real-time comparisons of air temperature and $\delta^{18}O$ measured on precipitation on the Northern Tibetan Plateau reveal a very close relationship between the two (Yao et al., 1996). Correlations between ice core records from the Himalayas and the Northern Hemisphere temperature records show that on longer time scales (longer than annual) the dominant factor controlling mean $\delta^{18}O$ values in snowfall must be temperature rather than precipitation (Thompson et al., 2000; Davis and Thompson, 2003). On seasonal to annual time scales, both temperature and precipitation influence the local $\delta^{18}O$ signal (Vuille et al., 2003).

The annual precipitation rate on an ice cap, or net balance, can be reconstructed by measuring the length of ice between seasonal variations in one or more parameters (e.g., $\delta^{18}O$ indicating warm or cold seasons or high aerosol concentrations characterizing dry seasons, Figure I4) Since ice is viscous, it

tends to flow not only horizontally but also vertically, resulting in annual layer thinning with depth. In order to correct for this deformation and reconstruct the original thickness of an annual layer at the time of its deposition in the past, vertical strain models are used that take into account the changing densities with depth, the thickness of the glacier, and the rate of thinning (Bolzan, 1985; Reeh, 1988; Meese et al., 1994).

Aerosols in the atmosphere are either deposited on mountain ice fields and glaciers as nuclei of snow (wet deposition) or carried by turbulent air currents to high altitudes (dry deposition). Either way, these insoluble mineral dust particles and soluble salts, such as chlorides, record variations in environmental conditions such as regional aridity. The concentration and size distribution of insoluble dust particles are also helpful for qualitative reconstructions of wind strength. Evidence of volcanic eruptions in the ice is provided by sulfate concentrations and/or the presence of microscopic tephra particles. If these volcanic layers are identifiable (e.g., the 1815 eruption of Tambora or the 1883 eruption of Krakatoa), they can serve as valuable reference horizons to calibrate the time scale. Biological aerosols, such as pollen grains (Liu et al., 1998) and nitrates that may have been injected into the atmosphere by vegetation upwind of a glacier (Thompson et al., 1995; Thompson, 2000), have been useful for reconstructing past climate and environmental changes that have had impacts on regional flora.

The record of human activity is also available from ice cores, although this type of research on high-altitude glaciers lags behind polar ice sheets. Research on heavy metal types and concentrations in high-altitude glaciers is relatively new, but what is available from Mont Blanc in the French-Italian Alps provides information about increasing industrial production and other activities associated with expanding populations and urbanization (Van DeVelde et al., 1999). Measurements of carbon dioxide and methane, as well as lesser gases, trapped in ice bubbles are not as extensive on ice from mountain glaciers as they are from polar cores; however, the research that has been done shows correlations of so-called "greenhouse" gas concentrations with the temperature proxy $\delta^{18}O$ (Yao et al., 2002a, b). The information from these ice core studies complements other proxy records that compose the Earth's climate history, which is the ultimate yardstick by which the significance of present and projected anthropogenic effects will be assessed.

The significance of climate records from mountain glaciers

Ice core records from high-altitude glaciers, when combined with high-resolution proxy histories such as those from tree rings, lacustrine and marine cores, corals, etc., provide an unprecedented view of the Earth's climatic history that can extend over several centuries or millennia. The longest of them have revealed the nature of climate variability since the Last Glacial Maximum (LGM), 18–20 thousand years ago, and even beyond. The more recent parts of the climate records, which are of annual and even seasonal resolution, can yield high-resolution temporal variations in the occurrence and intensity of coupled ocean-atmosphere phenomena such as El Niño and monsoons, which are most strongly expressed in the tropics and subtropics, and are of world-wide significance. This is particularly valuable information since meteorological observations in these regions are scarce and of short duration.

Four records from the Andes (Huascarán in Northern Peru, Coropuna in Southern Peru and Sajama and Illimani in Bolivia) and one from the Western Tibetan Plateau (Guliya) extend to or past the end of the last glacial stage and confirm, along with other climate proxy records (e.g., Guilderson et al., 1994; Stute et al., 1995), that the LGM was much colder in the tropics and subtropics than previously believed. Although this period was consistently colder, it was not consistently drier through the lower latitudes as it was in the polar regions. For example, the effective moisture along the axis of the Andes Mountains during the end of the last glacial stage was variable, being much drier in the north than in the Altiplano region in the central part of the range (Thompson et al., 1995, 1998; Ramirez et al., 2003). In another example in Western China, the Guliya Ice Cap is partly affected by the variability of the southwest Indian monsoon system, which was much weaker during the last glacial stage than during the Holocene. However, this region of the Tibetan Plateau also receives (and received) moisture generated from the cyclonic activity carried over Eurasia by the prevailing wintertime westerlies. Not only were lake levels in the Western Kunlun Shan higher than tropical lakes during the LGM (Li and Shi, 1992), but the dust concentrations in the Guliya ice core record were consistent with those of the Early Holocene when the summer Asian monsoons became stronger, suggesting that local sources of aerosols were inhibited during this cold period by higher precipitation and soil moisture levels (Davis, 2002).

Ice cores from the Andes can also contribute to what is known about past environmental and climatic conditions of the Amazon Basin. The extent of biological activity in the Amazon rainforest during the LGM is controversial, and the nitrate concentration record from the Huascarán ice core has been included in the argument (Colinvaux et al., 2000). Pollen studies from the Amazon Basin suggest that the extent of the rainforest has not changed much between the glacial maximum and the Holocene. However, proponents of the "refugia" theory (i.e., Clapperton, 1993) assert that the cold, dry climate in the tropics caused a major retreat of the rainforest flora into a small, geographically isolated area, leaving most of the Basin covered by grasslands. In the Huascarán core, the nitrate concentration profile is similar to the $\delta^{18}O$ levels throughout most of the record, and the very low concentrations of nitrate, which are concurrent with very depleted $\delta^{18}O$, suggest that biological activity upwind of the Cordillera Blanca was impeded by the cold and dry climate ~19,000 years ago.

Most of the deep cores from the low latitudes extend through at least the Holocene, and show spatial variations in climate, even between records from the same region. For example, the Holocene $\delta^{18}O$ profiles from Huascarán and Illimani, while similar to each other in that they show Early Holocene isotopic enrichment, are different from that on Sajama, which has a relatively stable isotopic record through the last 10,000 years. Although Sajama and Illimani, both in Bolivia, are geographically close to each other, they are on opposite sides of the Andean Mountains, with Illimani located in the eastern range. Like Huascarán far to the north, it received most of its precipitation from the northeast after it had been recycled through the Amazon Basin. Sajama, which is located on the high, dry Altiplano, is more subject to Pacific influences and local hydrological effects.

Holocene ice core records from mountain glaciers around the world show evidence of major climatic disruptions, such as droughts and abrupt cold events during this period, which previously was believed to have been stable. Major dust events, beginning between 4.2 and 4.5 ka and lasting several hundred years, are observed in the Huascarán and Kilimanjaro ice cores

(Thompson, 2000; Thompson et al., 2002, respectively), and the timing and character of the dust spikes are similar to one seen in a marine core record from the Gulf of Oman (Cullen et al., 2000) and a speleothem $\delta^{13}C$ record from a cave in Israel (Bar-Matthews et al., 1999). This dry period is also documented in several other proxy climate records throughout Asia and Northern Africa (see contributions in Dalfes et al., 1994). Two other periods of abrupt, intense climate change in east Africa are observed in the Kilimanjaro ice core at ~8.3 ka and 5.2 ka (Thompson et al., 2002). The latter event is associated with a sharp decrease in $\delta^{18}O$, indicative of a dramatic but short-term cooling.

More recently, a historically documented drought in India in the 1790s, which was associated with monsoon failures and a succession of severe El Niños, was recorded in the insoluble and soluble aerosol concentration records in the Dasuopu ice core (Thompson et al., 2000). Another recorded Asian Monsoon failure in the late 1870s (Lamb, 1982) is noticeable in the Dasuopu dust flux record, which is a calculation that incorporates both the dust concentration and the annual net balance. The dust concentration on Dasuopu is also linked to the magnitude of the Southern Oscillation and the phase of the Pacific Decadal Oscillation (Davis, 2002), thus indicating a linkage between these tropical processes. However, recent research on Tibetan Plateau ice cores drilled north of 32° N shows that their climate records are not only influenced by the South Asian Monsoon and other tropical coupled atmospheric-oceanic processes such as the El Niño-Southern Oscillation (ENSO), but also by atmospheric pressure variations such as those seen in the North Atlantic Oscillation (Davis and Thompson, 2003; Wang et al., 2004). Thus, the high resolution isotope, chemistry, dust, and accumulation records from ice cores retrieved from across the Plateau help us to reconstruct the spatial and temporal variability of the climate in this region.

There is little purpose in trying to reconstruct the history of global climate change from one ice core, especially at high resolution on short time scales. However, as discussed above, it is clear that certain parameters such as $\delta^{18}O$ do record large-scale regional variability in sea surface temperatures, while others such as aerosols may be more sensitive to local as well as regional conditions. Although the mountain ice core records that extend back through the last millennium show regional differences with each other and with the polar records, many of them also document common climatic variations on hemispheric, and even global, scales. This is illustrated in Figure I5, where composites of the decadally-averaged $\delta^{18}O$ profiles of three South American cores (Huascarán, Quelccaya, and Sajama) and three Tibetan Plateau cores (Dunde, Guliya and Dasuopu) show different interhemispheric trends (Thompson et al., 2003) (Figures I5a and I5b, respectively). For example, the "Little Ice Age," a cold event between the fifteenth and nineteenth centuries that is recorded in many Northern European climate records, is more evident in the South American ice core composite than in the Tibetan Plateau. The "Medieval Warming," a period before the "Little Ice Age," which appears in the Greenland ice core records, is also obvious in the Andean ice cores. However, both the composites show isotopic enrichment (indicating warming) beginning in the late nineteenth century and accelerating through the twentieth century. When all six of the profiles from these mountain glaciers are combined, the resulting composite (Figure I5c) is similar to the Northern Hemisphere temperature records of Mann et al. (1998) and Jones et al. (1998) covering the last 1,000 years (Figure I5d).

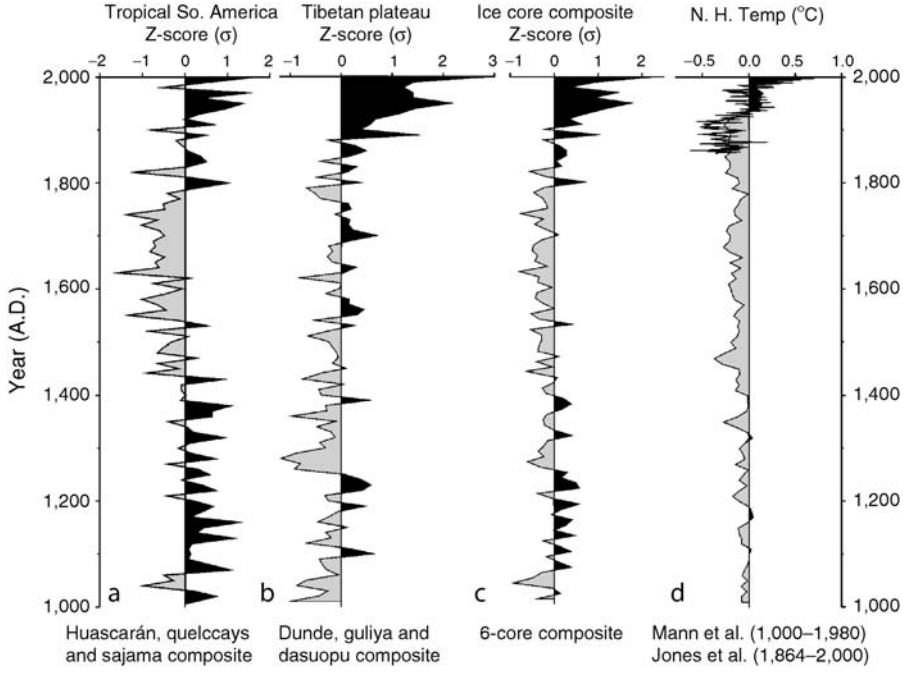

Figure I5 Composite records of decadal averages of $\delta^{18}O$ from ice cores from (**a**) the South American Andes (Huascarán, Quelccaya, Sajama) and (**b**) the Tibetan Plateau (Dunde, Guliya and Dasuopu) from 1000 AD to the present. All six ice-core records are combined (**c**) to give a total view of variations in $\delta^{18}O$ over the last millennium in the tropics, which is compared with the Northern Hemisphere reconstructed temperature record (**d**) (from Thompson et al., 2003).

Not only do these comparisons argue for the important role of temperature in the composition of oxygen isotopic ratios in glacier ice, but they also demonstrate that the abrupt warming from the late nineteenth century through the twentieth century (and continuing into this century) transcends regional variations, unlike earlier climatic variations. Indeed, on a global basis, the twentieth century was the warmest period in the last 1,000 years, which also encompasses the time of the "Medieval Warming."

The modern climate warming and its effects on mountain glaciers

Meteorological data from around the world suggest that the Earth's globally averaged temperature has increased 0.6° C since 1950. The El Niño year of 1998 saw the highest globally averaged temperatures on record, while 2002 (a non-El Niño year) was the second warmest, followed by 2003 and 2001 (a la Niña year). The recent warming of the past century, which has been accelerating in the last two decades, is recorded in alpine glaciers in other ways, both within the ice core records and by the rapid retreat of many of the ice fields. This glacier retreat is observed in almost all regions, from the Caucasus and other Eurasian mountain ranges in the mid-latitudes (Mikhalenko, 1997), to central Europe and western North America (Huggel et al., 2002; Meier et al., 2003), and to the Tibetan Plateau and the tropics (Thompson et al., 1993; Dahe et al., 2000; Thompson et al., 2000). In the Andes, on the Tibetan Plateau and in the East Africa Rift Valley region, this climate change has left its mark. The many ice fields on Kilimanjaro covered an area of 12.1 km^2 in 1912, but today only 2.6 km^2 remains (Figure I6). If the current rate of retreat continues, the perennial ice on this mountain will likely disappear within the next 20 years (Thompson et al., 2002).

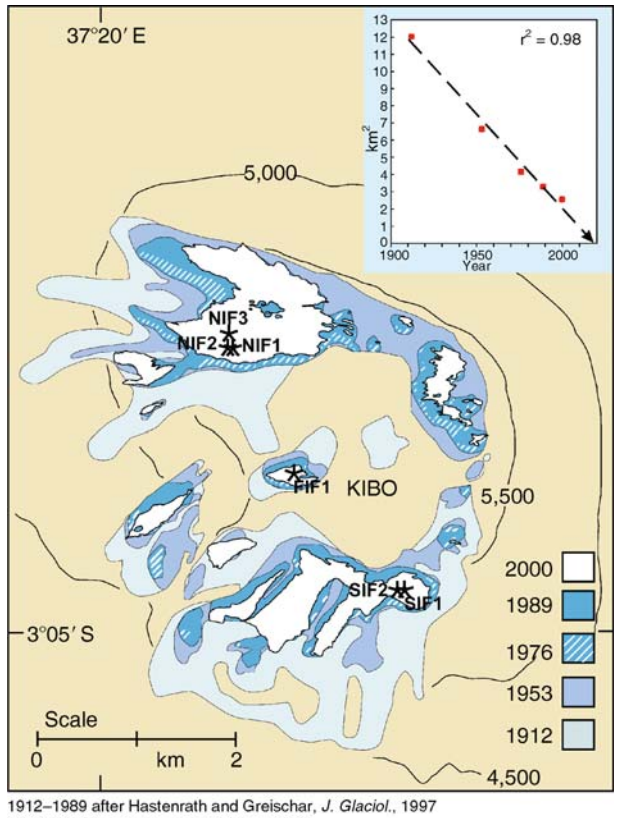

Figure I6 Retreat of ice fields in the Kibo Crater of Kilimanjaro, Tanzania. *Shaded areas* show "snapshots" of areas of ice cover at five times over the twentieth Century. At the rate of retreat shown here, all the ice on this mountain will disappear within the first half of the twenty first century (*insert*) (from Thompson et al., 2002).

Future priorities

Ice cores from mountain glaciers, especially those from the tropical and subtropical latitudes where most of the world's

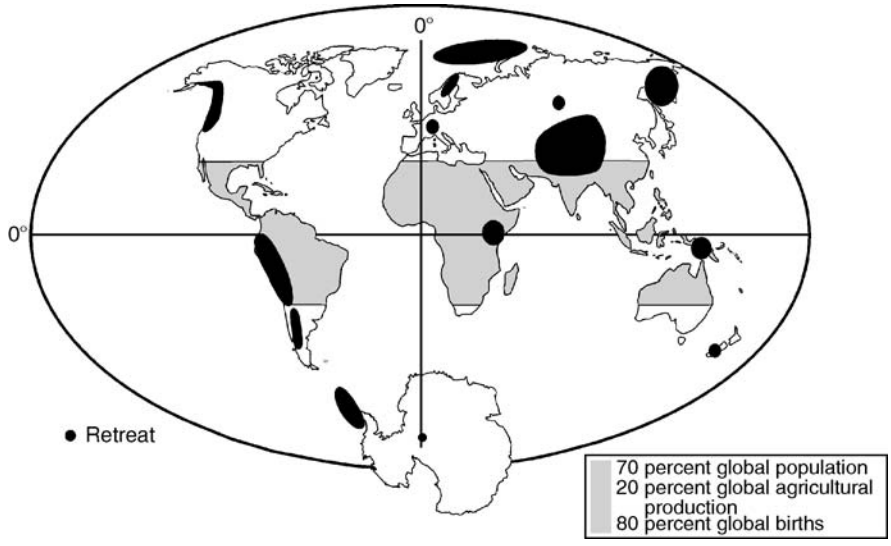

Figure I7 Map demonstrating the current condition of the Earth's cryosphere. *Dark shading* depicts regions where glacier retreat is underway. The light shading represents over land between 30° N and 30° S.

population is concentrated, provide unique and valuable archives of climate information because they are able to record variations in atmospheric chemistry and conditions. Since 1982, the El Niño-Southern Oscillation phenomenon has gained worldwide attention as populations and governments have come to realize the extent of its widespread and often devastating effects on weather. As we begin to understand how this coupled atmospheric-oceanic process works, we also see its linkages with other important systems such as the Asian/African Monsoons. Because both of these tropical systems influence precipitation and temperature over large regions, their effects are also recorded by the chemistry and the amount of snow that falls on alpine glaciers. Seasonal and annual resolution of chemical and physical parameters in ice core records from the Andes Mountains has allowed reconstruction of the variability of the ENSO phenomenon over several hundred years (Thompson et al., 1984, 1992; Henderson, 1996; Henderson et al., 1999). Because the effects of El Niño and La Niña events are spatially variable, ice core records from the northernmost (Colombia) and southernmost (Patagonia) reaches of the Andes Mountains will help further resolve the frequency and intensity of ENSO, along with temperature variations, from long before human documentation. This will aid in placing the modern climate changes and the modern ENSO into a more comprehensive perspective. Variability of the South Asian Monsoon is also of vital importance for a large percentage of the world's population that lives in the affected areas. Cores from the Tibetan Plateau have yielded millennial-scale histories of monsoon variability across this large region and information on the interaction between the monsoon system and the prevailing westerlies that are traced back to the Atlantic Ocean.

The clearest evidence for major climate warming underway today comes from the mountain glaciers, recorded in both the ice core records and in the drastic reductions in both total area and total volume. The rapid retreat causes concern for two reasons. First, these glaciers are the world's "water towers," and their loss threatens water resources necessary for hydroelectric production, crop irrigation and municipal water supplies for many nations. The ice fields constitute a "bank account" that is drawn upon during dry periods to supply populations downstream. The current melting is cashing in on that account, which was built over thousands of years but is not currently being replenished. As Figure I7 illustrates, almost all the Earth's mountain glaciers are currently retreating. The land between 30° N and 30° S, which constitutes 50% of the global surface area, is home to 70% of the world's population and 80% of the world's births. However, only 20% of the global agricultural production takes place in these climatically sensitive regions. The second concern arising from the disappearance of these ice fields is that they contain paleoclimatic histories that are unattainable elsewhere and, as they melt, the records preserved therein are forever lost. These records are needed to discern how climate has changed in the past in these regions and to assist in predicting future changes.

Lonnie G. Thompson

Bibliography

Baker, P.A., Seltzer, G.O., Fritz, S.C., Dunbar, R.B., Grove, M.J., Tapia, P.M., Cross, S.L., Rowe, H.D., and Broda, J.P., 2001. The history of South American tropical precipitation for the past 25,000 years. *Science*, **291**, 640–643.

Bar-Matthews, M., Ayalon, A., Kaufman, A., and Wasserburg, G.J., 1999. The Eastern Mediterranean paleoclimate as a reflection of regional events: Soreq Cave, Israel. *Earth Planet. Sci. Lett.*, **166**, 85–95.

Bolzan, J.F., 1985. Ice flow at the Dome C ice divide based on a deep temperature profile. *J. Geophys. Res.*, **90**(D5), 8111–8124.

Clapperton, C., 1993. *Quaternary Geology and Geomorphology of South America*, Amsterdam, The Netherlands: Elsevier, 779pp.

Colinvaux, P.A., DeOliveira, P.E., and Bush, M.B., 2000. Amazonian and neotropical plant communities on glacial time-scales: The failure of the aridity and refuge hypotheses. *Quaternary Sci. Rev.*, **19**, 141–170.

Cullen, H.M., deMenocal, P.B., Hemming, S., Hemming, G., Brown, F.H., Guilderson, T., and Sirocko, F., 2000. Climate change and the collapse of the Akkadian empire: Evidence from the deep sea. *Geology*, **28**, 379–382.

Dahe,Q., Mayewski, P.A., Wake, C.P., Shichang, K., Jiawen, R., Shugui, H., Tandong, Y., Qinzhao, Y., Zhefan, J., and Desheng, M., 2000. Evidence for recent climate change from ice cores in the central Himalaya. *Ann. Glaciol.*, **31**, 153–158.

Dalfes, H.N., Kukla, G., and Weiss, H. (eds.). 1994. Third Millennium BC Climate Change and Old World Collapse. Berlin: Springer, 723pp.

Dansgaard, W., 1961. The isotopic composition of natural waters with special reference to the Greenland Ice Cap. *Meddelelsr øm Grønland*, **165**, 1–120.

Davis, M.E., 2002. *Climatic Interpretations of Eolian Dust Records from Low-Latitude, High-Altitude Ice Cores*, The Ohio State University: PhD Thesis.

Davis, M.E., and Thompson, L.G., 2004. Four centuries of climatic variation across the Tibetan Plateau from ice-core accumulation and $\delta^{18}O$ records. In Cecil, L.D., Thompson, L.G., Steig, E.J., and Green, J.R. (eds.), *Earth Paleoenvironments: Records Preserved in Mid and Low Latitude Glaciers.* New York: Kluwer, pp 145–162.

Guilderson, T.P., Fairbanks, R.G., and Rubenstone, J.L., 1994. Tropical temperature variations since 20,000 years ago: Modulating interhemispheric climate change. *Science*, **263**, 663–665.

Hastenrath, S., and Greischar, L., 1994. Gacier recession on Kilimanjaro, East Africa, 1912–89. *J. Glaciol.* **43**, 455–459.

Henderson, K.A., 1996. *The El Niño-Southern Oscillation and other modes of Interannual Tropical Climate Variability as Recorded in Ice Cores from the Nevado Huascarán col, Peru*, The Ohio State University: M.S. Thesis.

Henderson, K.A., Thompson, L.G., and Lin, P.-N., 1999. Recording of El Niño in ice core $\delta^{18}O$ records from Nevado Huascarán, *Peru. J. Geophys. Res.*, **104**(D24), 31053–31065.

Huggel, C., Kaab, A., Haeberli, W., Teysseire, P., and Paul, F., 2002. Remote sensing based assessment of hazards from glacier lake outbursts: A case study in the Swiss Alps. *Can. Geotech. J.*, **39**(2), 316–330.

Jones, P.D., Briffa, K.R., Barnett,T.P., and Tett, S.F.B., 1998. High-resolution palaeoclimatic records for the last millennium: Interpretation, integration and comparison with general circulation model control-run temperatures. *Holocene*, **8**, 455–471.

Lamb. H.H., 1982. *Climate History and the Modern World*, London, UK: Methuen, 387pp.

Li, S., and Shi, Y., 1992. Glacial and lake fluctuations in the area of the west Kunlun Mountains during the last 45,000 years. *Ann. Glaciol.*, **16**, 79–84.

Liu, K.B., Yao, Z., and Thompson, L.G., 1998. A pollen record of Holocene climate changes from the Dunde ice cap, Qinghai-Tibetan Plateau. *Geology*, **26**(2), 135–138.

Mann, M.E., Bradley, R.S., and Hughes, M.K., 1998. Global-scale temperature patterns and climate forcing over the past six centuries. *Nature*, **392**, 779–787.

Meese, D.A., Gow, A.J., Grootes, P., Mayewski, P.A., Ram, M., Stuiver, M., Taylor, K.C., Waddington, E.D., and Zielinski, G.A., 1994. The accumulation record from the GISP2 core as an indicator of climate change throughout the Holocene. *Science*, **266**, 1680–1682.

Meier, M.F., Dyurgerov, M.B., and McCabe, G.J., 2003. The health of glaciers: Recent changes in glacier regime. *Clim. Change*, **59**(1–2), 123–135.

Mikhalenko, V.N., 1997. Changes in Eurasian glaciation during the past century: Glacier mass balance and ice-core evidence. *Ann. Glaciol.*, **24**, 283–287.

Ramirez, E., Hoffmann, G., Taupin, J.D., Francou, B., Ribstein, P., Caillon, N., Ferron, F.A., Landais, A., Petit, J.R., Pouyaud, B., Schotterer, U., Simoes, J.C., and Stievenard, M.A., 2003. A new Andean deep ice core from Nevado Illimani (6,350 m), Bolivia. *Earth Planet. Sci. Lett.*, **212** (3–4), 337–350.
Reeh, N., 1988. A flow-line model for calculating the surface profile and the velocity, strain-rate, and stress fields in an ice sheet. *J. Glaciol.*, **34**(116), 46–54.
Rozanski, K., Araguás-Araguás, L., and Gonfiantini, R., 1993. Isotopic patterns in modern global precipitation. In Swart, P.K., Lohmann, K.C., McKenzie, J., and Savin, S. (eds.), *Climate Change in Continental Isotopic Records.* Washington, D.C.: American Geophysical Union, pp. 1–36.
Shichang, K., Wake, C.P., Dahe, Q., Mayewski, P.A., and Tandong, Y., 2000. Monsoon and dust signals recorded in Dasuopu glacier, Tibetan Plateau. *J. Glaciol.*, **46**(153), 222–226.
Stute, M., Forster, M., Frischkorn, H., Serejo, A., Clark, J.F., Schlosser, P., Broecker, W.S., and Bonani, G., 1995. Cooling of tropical Brazil (5° C) during the last glacial maximum. *Science*, **269**, 379–383.
Thompson, L.G., 2000. Ice-core evidence for climate change in the Tropics: Implications for our future. *Quaternary Sci. Rev.*, **19**, 19–36.
Thompson, L.G., Mosley-Thompson, E., and Arnao, B.M., 1984. El Niño-Southern Oscillation events recorded in the stratigraphy of the tropical Quelccaya ice cap, Peru. *Science*, **226**, 50–52.
Thompson, L.G., Mosley-Thompson, E., and Thompson, P.A., 1992. Reconstructing interannual climate variability from tropical and subtropical ice-core records. In Diaz, H.F., and Markgraf, V. (eds.), *El Niño: Historical and Paleoclimatic Aspects of the Southern Oscillation.* Cambridge, UK: Cambridge University Press, pp. 295–322.
Thompson, L.G., Mosley-Thompson, E., Davis, M., Lin, P.-N., Yao, T., Dyurgerov, M., and Dai, J., 1993. "Recent warming": Ice core evidence from tropical ice cores with emphasis upon Central Asia. *Global Planet. Change*, **7**, 145–146.
Thompson, L.G., Mosley-Thompson, E., Davis, M.E., Lin, P.-N., Henderson, K.A., Cole-Dai, J., Bolzan, J.F., and Liu, K.-b., 1995. Late Glacial Stage and Holocene tropical ice core records from Huascarán, *Peru. Science*, **269**, 47–50.
Thompson, L.G., Davis, M.E., Mosley-Thompson, E., Sowers, T.A., Henderson, K.A., Zagorodnov, V.S., Lin, P.-N., Mikhalenko, V.N., Campen, R.K., Bolzan, J.F., Cole-Dai, J., and Francou, B., 1998. A 25,000 year tropical climate history from Bolivian ice cores. *Science*, **282**, 1858–1864.
Thompson, L.G., Yao, T., Mosley-Thompson, E., Davis, M.E., Henderson, K.A., and Lin, P.-N., 2000. A high-resolution millennial record of the South Asian Monsoon from Himalayan ice cores. *Science*, **289**, 1916–1919.
Thompson, L.G., Mosley-Thompson, E., Davis, M.E., Henderson, K.A., Brecher, H.H., Zagorodnov, V.S., Mashiotta, T.A., Lin, P.-N., Mikhalenko, V.N., Hardy, D.R., and Beer, J., 2002. Kilimanjaro ice core records: Evidence of Holocene climate change in tropical Africa. *Science*, **298**, 589–593.
fig 15
Thompson, L.G., Mosley-Thompson, E., Davis, M.E., Lin, P.-N., Henderson, K., and Mashiotta, T.A., 2003. Tropical glacier and ice core evidence of climate change on annual to millennial time scales. *Clim. Change*, **59**(1–2), 137–155.
Tian, L., Masson-Delmotte, V., Stievenard, M., Yao, T., and Jouzel, J., 2001. Tibetan Plateau summer monsoon northward extent revealed by measurements of water stable isotopes. *J. Geophys. Res.*, **106**(D22), 28081–28088
van De Velde, K., Ferrari, C., Barbante, C., Moret, I., Bellomi, T., Hong, S., and Boutron, C., 1999. A 200 year record of atmospheric cobalt, chromium, molybdenum, and antimony in high altitude alpine firn and ice. *Environ. Sci. Tech.*, **33**(20), 3495–3501.
Vuille, M., Bradley, R.S., Healy, R.,Werner, M., Hardy, D.R., Thompson, L.G., and Keiming, F., 2003. Modeling $\delta^{18}O$ in precipitation over the tropical Americas, Part II: Simulation of the stable isotope signal in Andean ice cores. *J. Geophys. Res.*, **108**(D6), 4175–4192.
Wang, N., Thompson, L.G., Davis, M.E., Mosley-Thompson, E., Tao, T., and Pu, J., 2003. Influence of variations in NAO and SO on air temperature over the northern Tibetan Plateau as recorded by $\delta^{18}O$ in the Malan ice core. *Geophys. Res Lett.*, **30**(22), 2167–2170.
Yao, T., Thompson, L.G., Mosley-Thompson, E., Yang, Z., Zhang, X., and Lin, P.N., 1996. Climatological significance of $\delta^{18}O$ in north Tibetan ice cores. *J. Geophys. Res.*, **101**(D23), 29531–29537.
Yao, T., Duan, K., Xu, B., Wang, N., Pu, J., Kang, S., Qin, X., and Thompson, L.G., 2002a. Temperature and methane changes over the past 1,000 years recorded in Dasuopu glacier (central Himalaya) ice core. *Ann. Glaciol.*, **35**, 379–383.
Yao, T., Thompson, L.G., Duan, K., Xu, B., Wang, N., Pu, J., Tian, L., Sun, W., Kang, S., and Qin, X., 2002b. Temperature and methane records over the last 2 ka in Dasuopu ice core. *Sci. China Ser. D: Earth Sci.*, **45**(12), 1068–1074.

Cross-references

Aerosol (Mineral)
Deuterium, Deuterium Excess
Ice Cores, Antarctica and Greenland
Little Ice Age
Medieval Warm Period
Monsoons, Quaternary
Mountain Glaciers
North Atlantic Oscillation (NAO) Records
Oxygen Isotopes
Paleo-El Niño-Southern Oscillation (ENSO) Records
Paleo-precipitation Indicators

"ICEHOUSE" (COLD) CLIMATES

Earth's climate has changed, within life-sustaining bounds, from warm to cool intervals, on scales from thousands to hundreds of millions of years. In the Phanerozoic Eon there have been three intervals of glaciation (Ordovician, Carboniferous and Cenozoic) lasting tens of millions of years, with ice down to sea level at mid-latitudes (Frakes et al., 1992; Crowell, 1999). These cool "icehouse" intervals were generally times of lower sea level, lower CO_2 percentage in the atmosphere, less net photosynthesis and carbon burial, and less oceanic volcanism than during alternating "greenhouse" intervals (Fischer, 1986). The transitions from Phanerozoic icehouse to greenhouse intervals were synchronous with some biotic crises or mass extinction events, reflecting complex feedbacks between the biosphere and the hydrosphere.

Figure I8 summarizes Earth's entire paleoclimate history, and Figure I9 shows the better-known Phanerozoic Eon, with carbon, strontium and sulfur isotopic ratios that are linked to major climate changes. Figure I10 shows an anti-correlation between atmospheric CO_2 levels and $\delta^{18}O$ values (proxy for oceanic temperature), which tracks the latitude of ice-rafted glacial debris.

The Cryogenian Period of Neoproterozoic time (about 750–580 Ma) contains rocks deposited in two or more severe Icehouse intervals (Harland, 1964; Knoll, 2000). Laminated cap carbonates with depleted $\delta^{13}C$ ratios are found on top of glacial marine diamictites in many successions (Kauffman et al., 1997). The sharp juxtaposition of icehouse versus greenhouse deposits has led some to suggest that rapid and extreme climate changes took place in Neoproterozoic time. The Snowball Earth hypothesis proposes that during these Neoproterozoic glaciations, the world ocean froze over. The cap carbonates are thought to have been deposited during a subsequent alkalinity event, caused by rapid warming and supersaturation of sea water on shallow continental shelves (Hoffman et al., 1998; Kennedy et al., 2001; Hoffman and Schrag, 2002).

The Earth's temperature has remained relatively constant for 3.8 by, within a range where life could exist (Figure I11), even though solar luminosity has increased and atmospheric

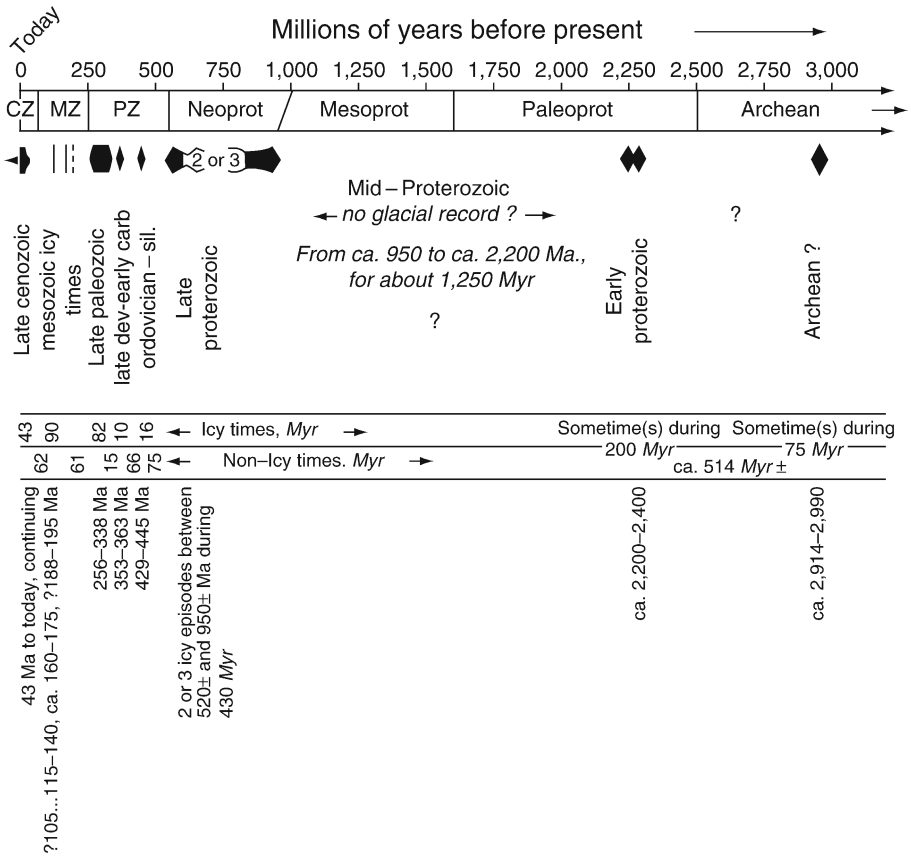

Figure I8 Major ice ages on Earth when the extent of continental glaciers was so great that tongues of ice reached the sea. Duration of icy andnon-icy times is shown in the middle of the figure. *CZ* = Cenozoic; *MZ* = Mesozoic; *PZ* = Paleozoic; *NEOPROT* = Neoproterozoic; *MESOPROT* = Mesoproterozoic; *PALEOPROT* = Paleoproterozoic (from Crowell, 1999, Figure 1, used by permission of Geological Society of America).

CO_2 levels have steadily decreased, since Archean time. In the Phanerozoic, the atmospheric CO_2 concentration has varied drastically between icehouse and greenhouse times (Figure I10) (Berner, 1990, 1991; Veizer, 2000; Crowley and Berner, 2001). These concentrations are buffered by feedback loops involving water vapor within the hydrosphere and complex relations in the biosphere (Kump, 2002).

Icehouse characteristics

In general, icehouse conditions occur at times of lower sea level, less cumulative volcanic activity, more vigorous oceanic circulation and bottom water oxidation, less diversity in marine organisms, and deeper levels of the carbonate compensation depth. Relatively warmer, greenhouse intervals are characterized by marine transgression, extensive carbonate bank systems, organic-rich shale basins, marine chert and phosphorite deposition, and nutrient upwelling (Fischer and Arthur, 1977). During icehouse intervals, several or all of the tectonic, geochemical, and astronomical events discussed below coincide. However, determination of the relative cause and effect of each factor, each with its own feedback system, is complex. Both terrestrial and celestial components are involved.

Glaciation to sea level at mid latitudes

The empirical definition of an icehouse state as seen in the geologic record is the presence of floating sea-ice at mid-latitudes (30°), and therefore the presence of ice-rafted debris (dropstones) in marine sediments (Frakes et al., 1992). Glacial ice has likely been present in high mountains throughout the Phanerozoic but the preservation potential of such alpine glacial deposits is low (Crowell, 1999) (see *Ice-rafted debris (IRD)*; *Glacial geomorphology*).

Well-mixed and colder oceans

During an icehouse, the deep ocean floor is oxygenated, and oceans are well-mixed. Icehouse conditions are favored when continental positioning allows north-south ocean circulation to bring warm equatorial water into polar latitudes where it evaporates and generates snowfall. This was the case during the Quaternary. Pleistocene oceanic bottom water temperatures were 15 °C lower than during the Mesozoic greenhouse (Crowley and Berner, 2001).

Carbon dioxide in atmosphere is lower

The percent of CO_2 in the atmosphere is lower in icehouse times, and generally tracks, and partly causes, the net change in temperature (Berner, 1990). Today's CO_2 percentage is in the icehouse range, at 300–370 ppm (Crowley and Berner, 2001). Models show this to be 17% of the Late Cretaceous greenhouse value, and perhaps only 5% of Cambrian Greenhouse CO_2 levels (Figure I10) (Chen and Drake, 1986; Berner, 1990). CO_2 percentage dropped with the Devonian advent of land plants and resulting accelerated silicate weathering.

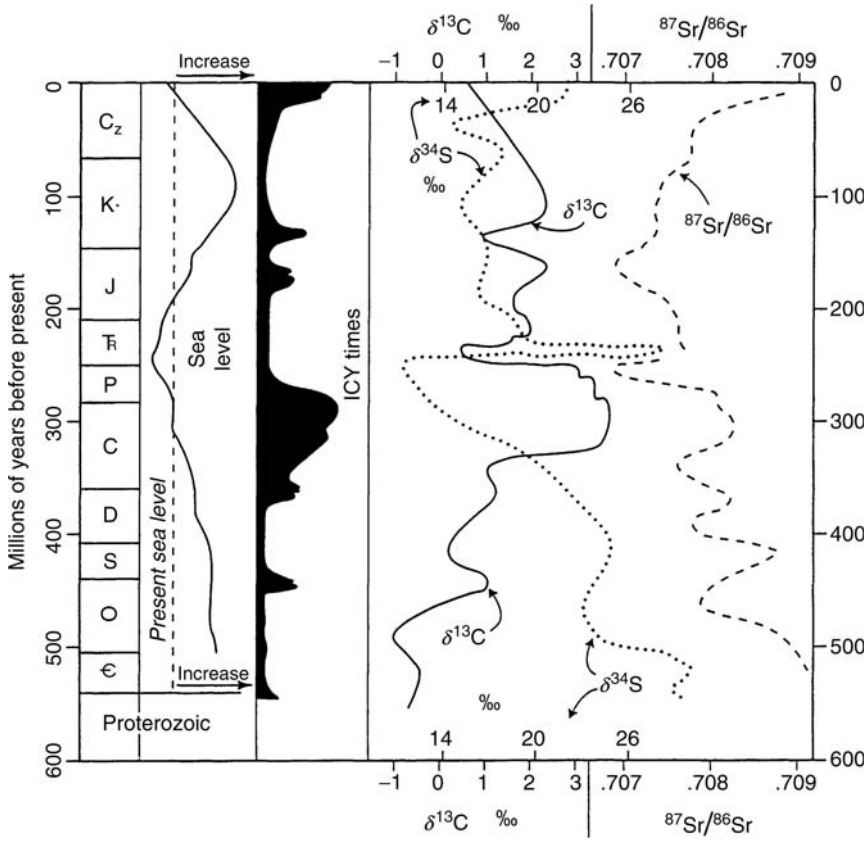

Figure I9 Carbon ($\delta^{13}C$), strontium ($^{87}Sr/^{86}Sr$), and sulfur ($\delta^{34}S$) isotopic ratios through Phanerozoic time compared with sea level and icy times. *Cz* = Cenozoic; *K* = Cretaceous; *J* = Jurassic; *Tr* = Triassic; *P* = Permian; *C* = Carboniferous; *D* = Devonian; *S* = Silurian; *O* = Ordovician; = Cambrian (from Crowell, 1999, Figure 25; originally modified from Veevers, 1994, Figure 1, used by permission of Geological Society of America).

Carbon isotope values are complex

Carbon is fractionated between organic matter (which is relatively concentrated in ^{12}C) and carbonate (inorganic) carbon (which is heavier in $\delta^{13}C$). Mantle carbon and methane (organic carbon) are both depleted in ^{13}C. The more sedimentary carbon that is buried as organic matter, the heavier will be the remaining carbonate carbon (Knoll, 1991). Further, increased weathering of sediments that contain isotopically light organic carbon, in orogenic belts, or from exposed continental shelves during times of low sea level, will shift the $\delta^{13}C$ ratio in carbonate sediments to more negative values.

In the Pleistocene, more negative $\delta^{13}C$ values correspond with times of greater glaciation. In the Neoproterozoic, major negative $\delta^{13}C$ spikes are found in carbonate rocks deposited on top of glacial marine sediments.

However, for the Late Paleozoic Ice Age and the Ordovician glaciation, $\delta^{13}C$ values are heavier than during the intervening greenhouse intervals (Figure I9). This apparent ambiguity has caused much controversy.

Global sea level is lower

Sea level is relatively lower during icehouse modes (Figure I9). At such times, water is stored in glacial ice, causing significant drops in global sea level on timescales of 10^5 yr (100 kyr). The extent of sea ice has an important positive feedback on the albedo or reflectivity of the Earth, which increases as sea level drops and ice expands. As the albedo increases, the Earth absorbs less solar radiation, and the climate becomes cooler. Conversely, during warmer, more humid times, sea level is high and polar ice is minimal, lowering the Earth's albedo. The ultimate long-term (10^8 years – first order) controls on sea level are tectonic, expressed as the average elevation of water-displacing, thermally inflated ocean floor, which is itself a function of the average rate of sea-floor spreading.

Bioherms and evaporites restricted to low latitude: aragonite seas

During icehouse intervals, bioherms and evaporites are restricted to less than 20° latitude. There is lower invertebrate diversity in high latitudes. Like today, aragonite and high-Mg calcite ooids precipitate in shallow marine environments (as opposed to low-Mg calcite ooids during greenhouse times) (Stanley and Hardie, 1998).

Reduced pelagic diversity

Diversity of the pelagic marine realm was reduced (oligotaxy) during icehouse intervals. Such oligotaxic times fostered intense blooms of opportunistic pelagic organisms at times of cumulative lowest diversity (Fischer and Arthur, 1977; Fischer, 1982, 1986).

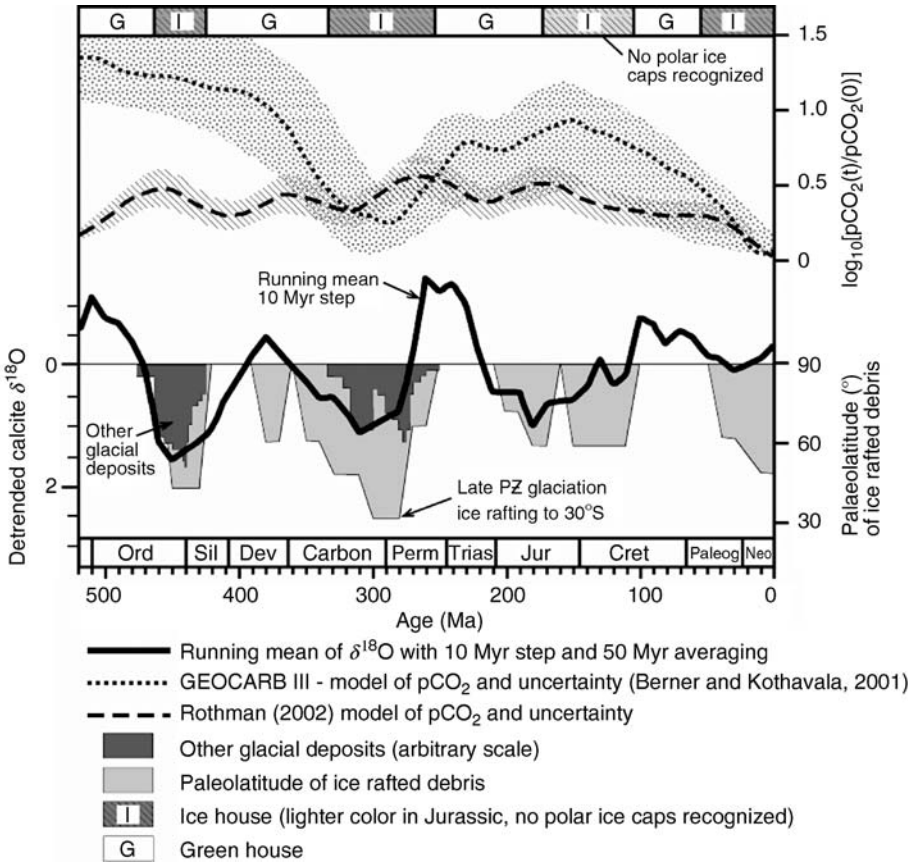

Figure I10 Phanerozoic climatic indicators and reconstructed pCO_2 levels (adapted from Shaviv and Veizer, 2003, Figure 1). Icehouse and greenhouse intervals are shown at the top of the diagram. *Upper two curves* represent estimated pCO_2 from the GEOCARB III CO_2 model (Berner and Kothavala, 2001) and the model of Rothman (2002). Oxygen isotope values from shells are shown with 10-Myr steps and 50-Myr averages. This smooths the curve and eliminates the highest readings. Paleolatitude of ice rafted debris and qualitative estimate of other glacial deposits are shown in the *lower part* of the diagram.

Carbonate compensation depth is deeper

During icehouse intervals, the CCD (carbonate compensation depth) is relatively deep within the world ocean, caused by the cooler oceanic temperatures and the resulting greater solubility of carbonate. Such conditions may not, however, apply to the Neoproterozoic, before the advent of pelagic carbonate-secreting organisms (Ridgwell et al., 2003).

Rates of carbon burial are reduced

In general, rates of carbon burial, or sequestration of organic carbon, are reduced in icehouse times, because the oceans are better aerated and the area of dysoxic restricted basins is smaller. The locations of such basins and associated carbon sinks are determined by plate configuration, global and local sea level, and by local organic productivity (controlled by upwelling). Low rates of accumulation of marine organic matter in Late Paleozoic time suggest well-ventilated Icehouse oceans.

Volcanic production of CO_2 is lower

In Phanerozoic cool periods, net production of CO_2 by volcanic activity is lower than during greenhouse events. Plate tectonic and mantle events cause these changes in net volcanic eruption rates, with decreased rates reflecting periods of supercontinents and slow sea-floor spreading.

Plate tectonic causation

Icehouse climates are favored during times of relatively slow sea-floor spreading, which, in the Phanerozoic, have been times of supercontinent persistence. In general, large continents favor formation of ice sheets (Frakes et al., 1992). For the Late Paleozoic and Late Cenozoic ice ages, a north-south arrangement of continents, fostering longitudinal ocean circulation, was a first-order cause of climate cooling.

A decrease in worldwide volcanic activity, with reduction in CO_2 emission, is controlled by the rate of sea-floor spreading. Such a decrease is favorable for a long-term icehouse event. Slower sea-floor spreading leads to lower global sea level, another icehouse characteristic.

Veevers (1990) suggests that supercontinent cycles are the ultimate cause of icehouse climates, which occur at times of maximum continentality and slower sea-floor spreading. Apparent long-term periodicities in global tectonic phenomena and impact cratering have been linked to motions of the solar system through the galaxy (e.g., Rampino and Stothers, 1986).

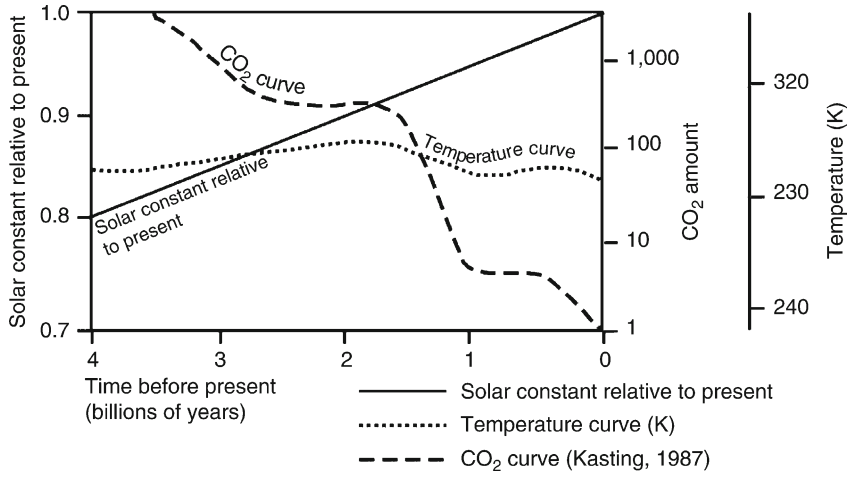

Figure I11 Variation of surface temperature, solar constant and atmospheric CO_2 over geologic time. Temperature curve refers to average surface temperature at 35° latitude. Note that CO_2 percentage has been falling steadily since the Archean, while solar output has been increasing. The net temperature has remained quite constant. Small-scale CO_2 changes, related to icehouse cycles, are superposed on this decreasing secular trend (simplified from Frakes et al., 1992, Figure 1.1).

However, Crowell (1999) does not recognize these tectonic supercycles. The presence or absence of deterministic chronotectonic supercontinent cycles is a recurring point of discussion in the study of Earth history.

Records of ancient glaciations

Glaciers are manifested differently at different latitudes, and include ice sheets, valley glacier and piedmont glacier complexes and mountain glaciers. Geological evidence for glaciation and glacial sedimentation are important to paleoclimatologists and sedimentologists, because they can indicate former cold climates (Harland, 1964; Deynoux et al., 1994; Crowell, 1999). Definitive ancient glacial deposits include poorly sorted diamictites, which may contain striated clasts and be associated with dropstone facies in proglacial lakes or seas (Link and Gostin, 1981).

A brief summary of the main icehouse intervals since 1,000 Ma follows. More detail is given in Crowell (1999).

Neoproterozoic (Cryogenian) glacial interval

Late Proterozoic glacial strata are found on all continents. The first evidence for ice sheets at low latitudes was marshaled by Harland (1964) who proposed the Great Infra-Cambrian ice age. Neoproterozoic paleocontinental positions suggest that most landmasses were at low latitudes, in areas of intense silicate weathering (Evans, 2000). This intense weathering traps carbonate and lowers global atmospheric CO_2 percentage (Kirschvink, 1992). Repeated studies have demonstrated low paleolatitudes for Neoproterozoic glacial marine strata (Sohl et al., 1999).

The Cryogenian Period of the Neoproterozoic is named for these icehouse intervals and has been investigated by the International Union of Geological Sciences (Knoll and Walter, 1992; Knoll, 2000; Narbonne, 2003).

Only recently have sufficiently accurate geochronologic data been obtained to place constraints on the Neoproterozoic glacial intervals, so that issues of synchroneity and extent of specific glacial advances remain controversial. Figure I12 shows the time and isotopic constraints, grouped into two broad icehouse intervals, Sturtian (730–670 Ma) and Marinoan (640–580 Ma), each tens of millions of years long in duration and each with several glaciations. The Marinoan glacial interval is used here in the inclusive sense (Knoll, 2000) to encompass the Varanger, Ghaub, and Gaskiers glaciations and is succeeded by the Ediacaran (Vendian) Period. New radiometric ages from glacial strata reveal multiple ages for ice advance, rather than two synchronous global ice ages (Bowring et al., 2003; Lund et al., 2003; Calver et al., 2004; Fanning and Link, 2004; Hoffmann et al., 2004; Zhou et al., 2004). Purely lithostratigraphic correlations have been a first start, but, to be credible, must be verified by geochronology.

Cap carbonates

Neoproterozoic glacial marine diamictites are often overlain by laminated cap carbonates that have strongly negative $\delta^{13}C$ values (e.g., Kauffman et al., 1997; Hoffman et al., 1998, Kennedy et al., 2001). Some cap carbonates contain spectacular aragonite crystal fans that grew rapidly on the sea floor. The juxtaposition of glacial (icehouse) deposits with carbonate (greenhouse) deposits is striking. In the Snowball Earth scenario, which proposes that the world oceans froze entirely over (Hoffman et al., 1998; Hoffman and Schrag, 2002), cap carbonates play an integral role and are thought to have been deposited rapidly during a post-glacial marine alkalinity event that was fed by a deeply weathered carbonate-rich regolith formed during the glaciation.

The severity of Cryogenian climate cycles is represented by the wide range of $\delta^{13}C$ values from Neoproterozoic carbonates (Figure I12) (Kaufman et al., 1997; Lorentz et al., 2004). Documented negative $\delta^{13}C$ isotopic excursions for carbonates immediately above the glacial rocks are as great as 16‰, going from + 10 to −6‰, which exceeds the magnitude of Phanerozoic excursions (Hoffman and Schrag, 2002). Levels of −6‰ suggest near-shutdown of the fractionation of ^{12}C in organic matter, as would happen with rapid deposition of shallow-marine carbonate during post-glacial transgression.

Crowell (1999) points out that these carbonates may not represent immediately warmed ocean water, but rather, slowly

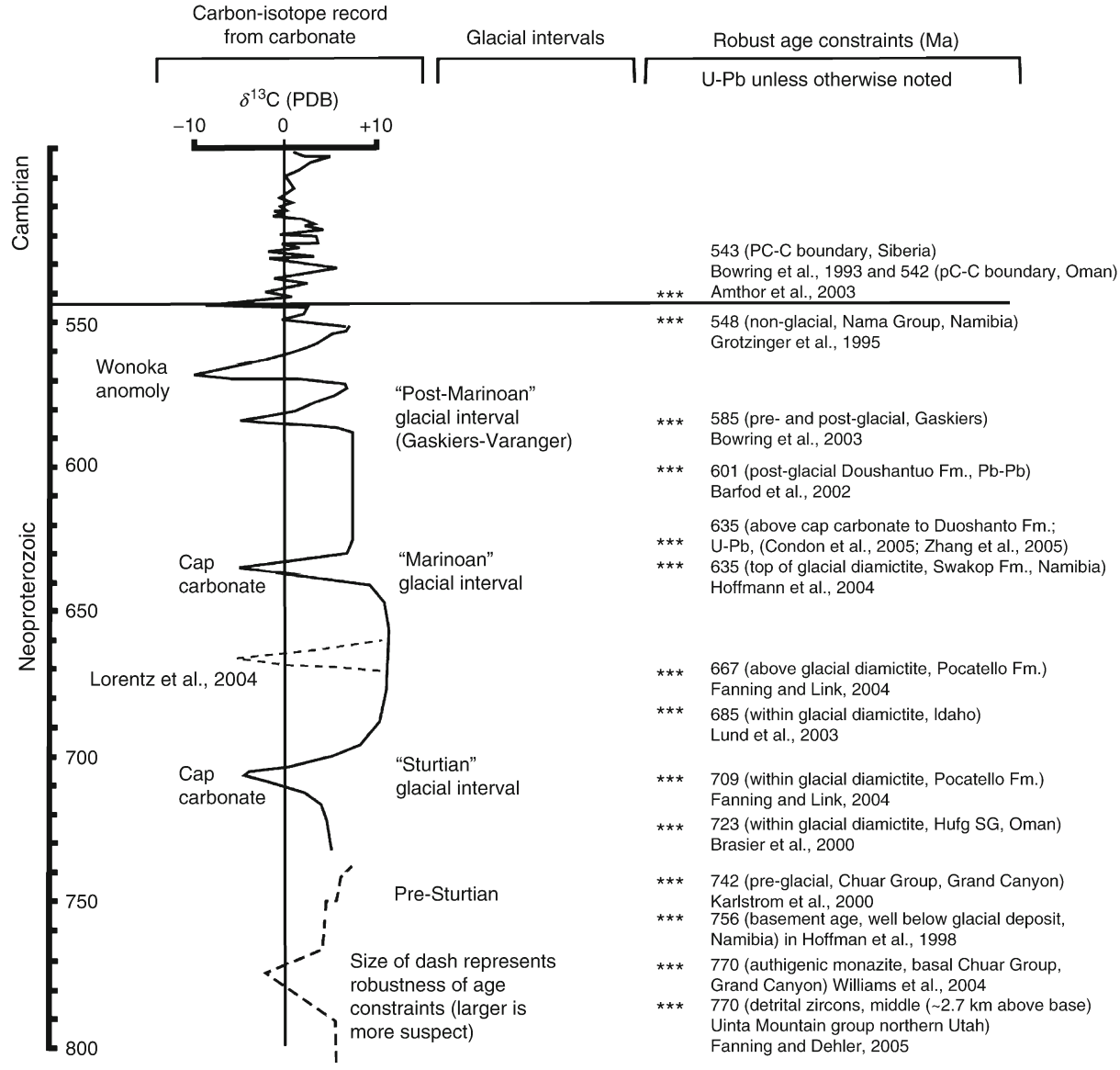

Figure I12 Late Neoproterozoic glacial intervals, carbon isotope values (Kaufman et al., 1997; Kennedy et al., 2001), and geochronologic constraints. Figure prepared by F. A. Corsetti, University of Southern California.

warming transgressive shelves above marine tillites. At least one post-glacial cap carbonate in south China has extremely low $\delta^{13}C$ values of −45‰, suggesting local methane release caused by post-glacial sea level rise and flooding of continental shelves (Jiang et al., 2003).

Proposed explanations of low-latitude Cryogenian glaciation

Low latitude glaciation has been explained by several hypotheses:

1. A climate system similar to that of today with unusual paleogeographic and tectonic factors combining to allow low-latitude glaciation;
2. A Snowball Earth with an ice shelf covering the ocean. (Note that a modification into a "Slushball Earth" may be necessary to account for evidence of meltwater during Neoproterozoic glaciations).
3. A greater inclination of Earth's spin axis such that polar regions have more equable climates than low-latitude positions (Williams, 1975);
4. True polar wander, where the lithosphere decouples from the asthenosphere and moves with respect to the magnetic field. This would cause inconsistent paleomagnetic pole positions on different continents;
5. Extraterrestrial influences, which may trigger climate cooling by the presence of abundant air-borne ejecta.

Late Ordovician and Early Silurian glaciations

During the Late Ordovician to early Silurian (~458–421 Ma), short but severe glaciations affected areas of South Africa,

the Saharan region of North Africa, and South America as the continents drifted over the South Pole. These glaciations were primarily due to continental positioning, and did not represent a global icehouse event. Atmospheric CO_2 percentage was high (Figure I10), but its effects were overridden by favorable continental positioning of Gondwanaland near the South Pole (Crowley and Berner, 2001).

Late Devonian and Early Carboniferous glaciations

Late Devonian and Early Carboniferous ice ages are recognized in isolated places in Brazil, in what were then high southern polar latitudes. Crowell (1999) includes these in his major episodes of glaciation, though Frakes et al. (1992) do not do so.

Late Paleozoic ice age

The Late Paleozoic ice age, from early Carboniferous to late Permian time (Figure I13) (~350–253 Ma) is the period of the well-known Gondwanan glaciations. It produced striated surfaces and tillites on all Gondwanan continents (Australia, India, Asia, Antarctica, South America and Africa). Glaciers extended away from the South Pole as far as 40° S latitude. In most places, several advance and retreat cycles can be recognized, and they are diachronous on different continents, tracking movement through high southern latitudes. In the Northern Hemisphere, glacio-eustatic cyclothems are recognized in the North American mid-continent. Gondwanan glacial deposits were part of the evidence used by Wegener for continental drift. Stones derived from southern and western Africa are found in glacial deposits in Brazil and Argentina.

The Late Paleozoic ice ages ended at least 5 Myr before the mass extinction at the end of the Permian. The warming process may have been facilitated by the outpouring of the Siberian trap lavas and associated CO_2 emission (see *Glaciations, pre-Quaternary*; *Late Paleozoic climates*).

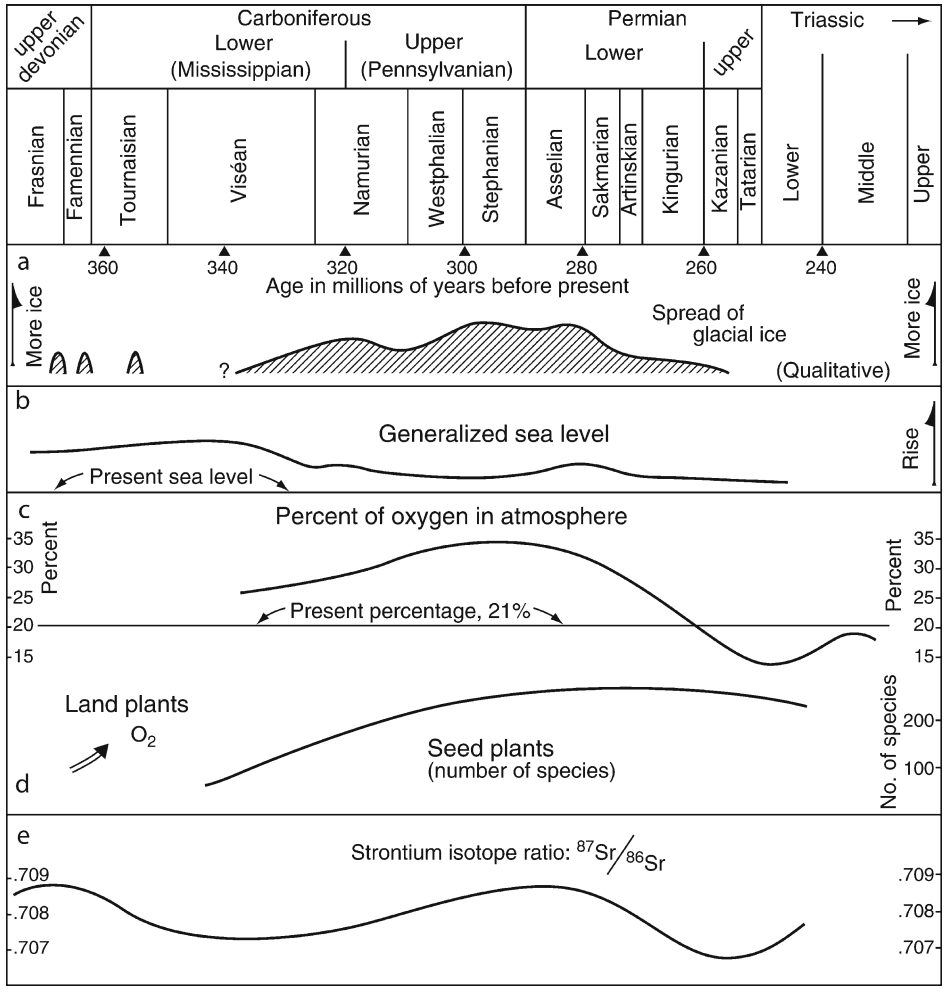

Figure I13 Time plot of glacial expansions during the Late Paleozoic ice ace from Devonian through Triassic time. Figure shows several possible cause and effect factors related to glacial advances. Geologic time scale calibrations from Harland et al. (1990), generalized sea-level curve from Vail et al. (1977), percent of oxygen in atmosphere from Berner (1990), number of species of land plants from Niklas et al. (1985), strontium isotopic ratios simplified from Burke et al. (1982) and Holser et al. (1988) (from Crowell, 1999, Figure 39; used with permission of the Geological Society of America).

Late Cenozoic ice age

The Late Cenozoic, Eocene to Recent glaciation (~55–0 Ma) (Frakes et al., 1992) began slowly and locally in the Antarctic. Ice-rafted sediment is present in 35 Ma Antarctic sediments. Worldwide cooling ensued by early Miocene time (22 Ma). Northern Hemisphere climates got progressively colder, as reflected by paleobotanical records of the southward migration of the extent of broad-leafed evergreen vegetation. The Cenozoic rise of the Himalayas intensified the Indian monsoon, and affected climate in numerous ways, including favoring Arctic cooling. The collision of India and Asia also created a CO_2 sink, due to enhanced chemical weathering of the uplifted Himalayan orogenic belt, which removed CO_2 from the atmosphere (see *Mountain uplift and climate change*). The greatest extent of glaciation was reached in the Pleistocene. Pleistocene climate cyclicity is recorded in $\delta^{18}O$ curves as measured from $CaCO_3$ shells of foraminifera, with the $\delta^{18}O$ values inversely related to ocean-water temperature (i.e., positive values indicate cold ocean temperatures and vice-versa; see *Oxygen isotopes*). Pleistocene glacial cyclicity generally follows Milankovich astronomical controls (see *Astronomical theory of climate change*; *Pleistocene climates*; *Glaciations, Quaternary*).

Summary

Earth has undergone several Icehouse periods, with the Pleistocene being the most recent. The controlling factors are both cyclic (external or astronomical) and secular (internal to the Earth), largely the product of plate tectonics (see *Climate change, causes*). In his synthesis of pre-Mesozoic ice ages, Crowell (1999) sees an irregular pattern of major glaciations, caused by changes in paleogeography and driven by plate tectonics, with secondary atmospheric and astronomical influence.

Earth's orbital variations are surely cyclic: "Allocyclic sedimentary rhythms – driven by orbital reaction of the Earth with this moon, its sibling planets, and the Sun, and transmitted through climate – are real" (Fischer, 1986). Luckily for us, Earth's history of extraterrestrial interactions has not fundamentally disrupted the life-sustaining Earth-Ocean-Lithosphere system. As shown in Figure I11, Earth's surface temperature has remained relatively constant within limits since the Archean, even though the luminosity of the Sun has increased and the amount of CO_2 in the atmosphere has decreased. Water vapor has acted as a buffer and climate moderator (Kump, 2002; Shaviv and Veizer, 2003).

CO_2 cycling through the biosphere is internal to the climate system, and thus cannot drive a secular change through time, but does affect feedbacks (see *Carbon cycle*). Net volcanism, related to sea-floor spreading rate, is an external forcing factor to the climate system, and had a major effect on the levels of CO_2 during the Mesozoic Greenhouse period (Kump, 2002). Even though the burning of fossil fuels has caused atmospheric CO_2 concentration to rise steadily since observations on Mauna Kea began in 1958 (Chen and Drake, 1986), changes in climate owing to human activity are geologically ephemeral. In taking a long-time view of the Earth's history, they represent but a quick excursion.

Paul K. Link

Bibliography

Amthor, J.E., Grotzinger, J.P., Schroeder, S., Bowring, S.A., Ramezani, J., Martin, M.W., and Matter, A., 2003. Extinction of Cloudina and Namacalathus at the Precambrian-Cambrian boundary in Oman. *Geology*, **31**, 431–434.

Barfod, G.H., Albarede, F., Knoll, A.H., Xiao, S., Telouk, P., Frei, R., and Baker, J., 2002. New Lu-Hf and Pb-Pb age constraints on the earliest animal fossils. *Earth Planet. Sci. Lett.*, **201**, 203–212.

Berger, W.H., 1982. Climate steps in ocean history—Lessons from the Pleistocene. In Berger, W.H., Crowell, J.C., et al. (eds), *Climate in Earth History, Studies in Geophysics.* Washington, DC: National Academy Press, pp. 43–54.

Berner, R.A., 1990. Atmospheric carbon dioxide levels over Phanerozoic time. *Science*, **249**, 1382–1386.

Berner, R.A., 1991. A model of atmospheric CO_2 over Phanerozoic time. *Am. J. Sci.*, **291**, 339–376.

Berner, R.A., and Kothavala, Z., 2001. GEOCARB III: A revised model of atmospheric CO_2 over Phanerozoic time. *Am. J. Sci.*, **301**, 182–204.

Bowring, S., Myrow, P., Landing, E., Ramezani, J., and Grotzinger, J., 2003. Geochronological constraints on terminal Neoproterozoic events and the rise of Metazoans. *Geophys. Res. Abstr.*, **5**, 13,219.

Brasier, M., McCarron, G., Tucker, R., Leather, J., Allen, P., and Shields, G., 2000. New U-Pb zircon dates for the Neoproterozoic Ghubrah glaciation and for the top of the Huqf Supergroup, Oman. *Geology*, **28**, 175–178.

Burke, W.H., Denison, R.E., Hetherington, E.A., Koepnick, R.B., Nelson, H.F., and Otto, J.B., 1982. Variations of seawater $^{87}Sr/^{86}Sr$ throughout Phanerozoic time. *Geology*, **10**, 516–519.

Calver, C.R., Black, L.P., Everard, J.L., and Seymour, D.B., 2004. U-Pb zircon age constraints on late Neoproterozoic glaciation in Tasmania. *Geology*, **32**, 893–896.

Chen, C.-T.A., and Drake, E.T., 1986. Carbon dioxide increase in the atmosphere and oceans and possible effects on climate. *Annu. Rev. Earth Planet. Sci.*, **14**, 201–236.

Condon, D., Zhu, M., Bowring, S., Wang, W., Yang, A., and Jin, Y., 2005. U-Pb ages from the Neoproterozoic Doushantuo Formation, China. *Science*, **308**, 95–98.

Crowell, J.C., 1999. *Pre-Mesozoic Ice Ages: Their Bearing on Understanding the Climate System.* 192, Boulder, CO: Geological Society of America Memoir 106pp.

Crowley, T.J., and Berner, R.A., 2001. CO_2 and climate change. *Science*, **292**, 870–872.

Deynoux, M., Miller, J.M.G., Domack, E.W., Eyles, N., Fairchild, I.J., and Young, G.M. (eds.), 1994. Earth's Glacial Record. Cambridge, UK: Cambridge University Press, 266pp.

Evans, D.A.D., 2000. Stratigraphic, geochronological, and paleomagnetic constraints upon the Neoproterozoic climatic paradox. *Am. J. Sci.*, **300**, 347–433.

Fanning, C.M., and Dehler, C.M., 2005, Constraining depositional ages for Neoproterozoic siliciclastic sequences through detrital zircon ages: A ca. 770 maximum age for the lower Uinta Mountain Group. *Geological Society of America Abstracts with Programs*, 37.

Fanning, C.M., and Link, P.K., 2004. 700 Ma U-Pb SHRIMP ages for Neoproterozoic (Sturtian) glaciogenic Pocatello Formation, southeastern Idaho. *Geology*, **32**, 881–884.

Fischer, A.G., 1982. Long-term climatic oscillations recorded in stratigraphy. In Berger, W. (ed.), *Climate in Earth History.* National Research Council, Studies in Geophysics, Washington, DC: National Academy Press, pp. 97–104.

Fischer, A.G., 1986. Climatic rhythms recorded in strata. *Annu. Rev. Earth Planet. Sci.*, **14**, 351–376.

Fischer, A.G., and Arthur, M.A., 1977. Secular variations in the pelagic realm. In Cook, H.C., and Enos, P. (eds.), *Deep Water Carbonate Environments.* SEPM Special Publication 25, pp. 18–50.

Frakes, L.A., Francis, J.E., and Syktus, J.I., 1992. *Climate modes of the Phanerozoic*. New York: Cambridge University Press, 274pp.

Grotzinger, J.P., Bowring, S.A., Saylor, B.Z., and Kaufman, A.J., 1995. Biostratigraphic and geochronologic constraints on early animal evolution. *Science*, **270**, 598–604.

Harland, W.B., 1964. Critical evidence for a great infra-Cambrian glaciation. *Geologische Rundschau*, **54**, 45–91.

Harland, W.B., Armstrong, R.L., Cox, A.V., Craig, L.E., Smith, A.G., and Smith, D.G. (eds.), 1990. A Geologic Time Scale 1989. Cambridge, UK: Cambridge University Press, 263pp.

Hoffman, P.F., and Schrag, D.P., 2002. The snowball Earth hypothesis: testing the limits of global change. *Terra Nova*, **14**, 129–155.

Hoffman, P.F., Kaufman, A.J., Halverson, G.P., and Schrag, D.P., 1998. A Neoproterozoic snowball Earth. *Science*, **281**, 1342–1346.

Hoffmann, K.-H., Condon, D.J., Bowring, S.A., and Crowley, J.L., 2004. U-Pb zircon date from the Neoproterozoic Ghaub Formation, Namibia: Constraints on Marinoan glaciation. *Geology*, **32**, 817–820.
Holser, W.T., Schidlowski, M., Mackenzie, F.T., and Maynard, J.B., 1988. Biogeochemical cycles of carbon and sulfur. In Gregor, C.B., Garrels, R.M., Mackenzie, F.T., and Maynard, J.B. (eds.), *Chemical Cycles in the Evolution of the Earth.* New York: Wiley, pp. 105–173.
Jiang, G., Kennedy, M.J., and Christie-Blick, N., 2003. Stable isotopic evidence for methane seeps in Neoproterozoic postglacial cap carbonates. *Nature*, **426**, 822–826.
Karlstrom, K.E., Bowring, S.A., Dehler, C.M., Knoll, A.H., Porter, S.M., DesMarais, D.J., Weil, A.B., Sharp, Z.D., Geissman, J.W., Elrick, M.B., Timmons, J.M., Crossey, L.J., and Davidek, K.L., 2000. Chuar Group of the Grand Canyon: Record of breakup of Rodinia, associated change in the global carbon cycle, and ecosystem expansion by 740 Ma. *Geology*, **28**, 619–622.
Kasting, J.F., 1987. Theoretical constraints on oxygen and carbon dioxide concentrations in the Precambrian atmosphere. *Precambrian Res.*, **34**, 205–229.
Kaufman, A.J., Knoll, A.H., and Narbonne, G.M., 1997. Isotopes, ice ages, and terminal Proterozoic Earth history. *Proc. Natl. Acad. Sci.*, **94**, 6600–6605.
Kennedy, M.J., Christie-Blick, N., and Sohl, L.E., 2001. Are Proterozoic cap carbonates and isotopic excursions a record of gas hydrate destabilization following Earth's coldest intervals? *Geology*, **29**, 443–446.
Kirschvink, J.L., 1992. Late Proterozoic low-latitude global glaciation: The snowball Earth, In Schopf, J.W., and Klein, C. (eds.), *The Proterozoic biosphere.* New York: Cambridge University Press, pp. 51–52.
Knoll, A.K., 1991, End of the Proterozoic Eon. *Sci. Am.*, **265**, 64–73.
Knoll, A.K., 2000. Learning to tell Neoproterozoic time. *Precambrian Res.*, **100**, 3–20.
Knoll, A.H., and Walter, M.R., 1992. Latest Proterozoic stratigraphy and Earth history. *Nature*, **356**, 673–677.
Kump, L.R., 2002. Reducing uncertainty about carbon dioxide as a climate driver. *Nature*, **419**, 188–190.
Link, P.K., and Gostin, V.A., 1981. Facies and paleogeography of Sturtian glacial strata (Late Precambrian), South Australia. *Am. J. Sci.*, **281**, 353–374.
Lorentz, N.J., Corsetti, F.A., and Link, P.K., 2004. Seafloor precipitates and C-isotope stratigraphy from the Neoproterozoic Scout Mountain Member of the Pocatello Formation, southeast Idaho: implications for Earth System behavior. *Precambrian Res.*, **130**, 57–70.
Lund, K., Aleinikoff, J.N., Evans, K.V., and Fanning, C.M., 2003. SHRIMP U-Pb geochronology of Neoproterozoic Windermere Supergroup, central Idaho: Implications for rifting of western Laurentia and synchroneity of Sturtian glacial deposits. *Geol. Soc. Am. Bull.*, **115**, 349–372.
Narbonne, G.M., 2003. I.U.G.S. Subcommission on the Terminal Proterozoic System, 18th circular (September 2003). http://geol.queensu.ca/people/narbonne/trm-prot/ (June 2004).
Niklas, K.J., Tiffney, B.H., and Knoll, A.H., 1985. Patterns in vascular land plant diversification: an analysis at the species level. In Valentine, J.W. (ed.), *Phanerozoic Diversity Patterns: Profiles in macroevolution.* Princeton, NJ: Princeton University Press, pp. 97–128.
Parrish, J.T., 1982. Upwelling and petroleum source beds, with reference to the Paleozoic. *AAPG Bull.*, **66**, 750–774.
Rampino, R., and Stothers, R.B., 1986. Geological periodicities and the galaxy. In Smoluchowski, R., Bahcall, J.N., and Matthews, M.S. (eds.), *The Galaxy and the Solar System.* Tucson, AZ: University of Arizona Press, pp. 241–259.
Ridgwell, A.J., Kennedy, M.J., and Calderia, K., 2003. Carbonate deposition, climate stability, and Neoproterozoic ice ages. *Science*, **302**, 859–862.
Rothman, D.H., 2002. Atmospheric carbon dioxide levels for the last 500 million years. *Proc. Natl. Acad. Sci.*, **99**, 4167–4171.
Shaviv, N.R., and Veizer, J., 2003. Celestial driver of Phanerozoic climate? *GSA Today*, **13**, 4–10.
Sohl, L.E., Christie-Blick, N.M., and Kent, D.V., 1999. Paleomagnetic polarity reversals in Marinoan (ca. 600 Ma) glacial deposits of Australia: implications for the duration of low-latitude glaciations in Neoproterozoic time. *Geol. Soc. Am. Bull.*, **111**, 1120–1139.
Stanley, S.M., and Hardie, L.A., 1998. Secular oscillations in the carbonate mineralogy of reef-building and sediment-producing organisms driven by tectonically forced shifts in seawater chemistry. *Palaeogeogr. Palaeoclimatol. Palaeoecol.*, **144**, 3–19.
Vail, P.R., Mitchum, R.M. Jr., Todd, R.G., Widmier, J.M., Thompson, S., III, Sangree, J.B., Bubb, J.N., and Hatlelid, W.G., 1977. Seismic stratigraphy and global changes of sea level. In Payton, C.E. (ed.), 26, *Seismic stratigraphy—Application to Hydrocarbon Exploration.* Tulsa, OK: American Association of Petroleum Geologists Memoir pp. 29–212.
Veevers, J.J., 1990. Tectonic-climatic supercycle in the billion-year plate-tectonic eon: Permian Pangean icehouse alternates with Cretaceous dispersed continent Greenhouse. *Sediment. Geol.*, **68**, 1–16.
Veevers, J.J., 1994. Pangea: Evolution of a supercontinent and its consequences for Earth's paleoclimate and sedimentary environments. In Klein, G.D. (ed.), *Geological Society of America Special Paper* 288, *Pangea: Paleoclimate, Tectonics, and Sedimentation During Accretion, Zenith, and Breakup of a Supercontinent.* Boulder, CO: Geological Society of America, pp. 13–23.
Veizer, J., Godderis, Y., and Francois, L.M., 2000. Evidence for decoupling of atmospheric CO_2 and global climate during the Phanerozoic eon. *Nature*, **408**, 698–701.
Williams, G.E., 1975. Late Precambrian glacial climate and the Earth's obliquity. *Geol. Mag.*, **112**, 441–444.
Williams, M. and 2004. Dating sedimentary sequences: in situ U/Th-Pb microprobe dating of early diagenetic monazite and Ar–Ar dating of marcasite nodules: Case studies from Neoproterozoic black shales in the southwestern U.S. *Geological Society of America Abstracts with Programs*, **35**, 595.
Worsley, T.R., Nance, R.D., and Moody, J.B., 1986. Tectonic cycles and the history of the Earth's biogeochemical and paleooceanic record. *Paleooceanography*, **1**, 233–263.
Zhang, S., Jiang, G., Zhang, J., Song, B., Kennedy, M.J., and Christie-Blick, N., 2005. U-Pb sensitive high-resolution ion microprobe ages from the Doushantuo Formation in south China: Constraints on late Neoproterozoic glaciations. *Geology*, **33**, 473–476.
Zhou, C., Tucker, R.D., Xiao, S., Peng, Z., Yuan, X., and Chen, Z., 2004. New constraints on the ages of Neoproterozoic glaciations in south China. *Geology*, **32**, 437–440.

Cross-references

Albedo Feedbacks
Astronomical Theory of Climate Change
Carbon Cycle
Carbon Isotope Variations over Geologic Time
Carbon Isotopes, Stable
Cenozoic Climate Change
Climate Change, Causes
Glacial Geomorphology
Glaciations, Pre-Quaternary
Glaciations, Quaternary
Greenhouse (warm) Climates
Ice-rafted Debris (IRD)
Late Paleozoic Paleoclimates (Carboniferous-Permian)
Mountain Uplift and Climate Change
Oxygen Isotopes
Plate Tectonics and Climate Change
Sea Level Change, Last 250 Million Years
Snowball Earth Hypothesis

ICE-RAFTED DEBRIS (IRD)

Introduction

Ice-rafted debris (IRD) is sediment of any grain size that has been transported by floating ice and released subsequently into an aqueous environment; the ice acts as a raft, providing buoyancy to any debris included within it or on its surface. Although IRD is often assumed to be transported by icebergs, the ice raft can be in the form of either icebergs, derived from

glaciers and ice sheets, or from sea ice formed by the freezing of sea water. IRD is usually deposited by icebergs and sea ice floating in marine waters, but icebergs, lake and river ice can also transport debris and release it subsequently into lakes.

Sources and distribution of debris

The best-known source of IRD is from glaciers and ice sheets. This form of IRD is heterogeneous in grain size, ranging from fine clays and silts to large boulders. This is because glacier ice can erode and transport material of all grain sizes. Sediments produced in the zone of shearing and crushing at the base of an ice sheet often show microscopic and larger edge rounding, together with striations and faceting of their surfaces. The modal shape class of this debris is sub-rounded in terms of Powers' visual roundness index. Such basally-derived glacial debris is usually found in the lowermost few centimeters to meters of glacier ice, at concentrations ranging from a few percent to a few tens of percent (Anderson et al., 1980). It can be present at higher levels in a glacier, usually in discrete bands of debris-rich ice, as a result of glaciotectonic processes such as folding and thrusting.

By contrast, debris incorporated at the glacier surface is usually derived from either rockfall or dirty-snow avalanching onto the ice, although finer-grained material can be deposited by the action of wind. Rockfall and avalanche debris is produced predominantly from weathering of exposed rock on valley walls, and is often relatively coarse-grained and angular in shape, with a sub-angular or angular modal Powers' roundness. Wind-blown debris is of silt and clay size, and is well sorted. Except locally, where significant rockfalls and avalanches have taken place, most of the debris load of glaciers is of basally-derived debris that is eroded or reworked at the glacier bed (Dowdeswell, 1986).

Sea ice also provides a vehicle for the long-distance ocean transport of sediments, although its load is typically of fine-grained material with rather few large clasts (Nürnberg et al., 1994). Fine sediments, entrained in shallow waters during storms, are incorporated when the sea-surface freezes during winter (Barnes et al., 1982). In addition, sediments can be entrained from the sea floor where the ice contacts it in shallow water, or where supercooled water freezes at the sea bed and entrains debris – such anchor ice can incorporate sand and coarser debris. Finally, debris can be introduced to the sea-ice surface through delivery by wind action or from the sediment load of rivers which can flow across shorefast sea ice during spring melting.

Debris release by melting and dumping

Icebergs are formed when ice breaks off, or calves, from the marine or lake margins of glaciers and ice sheets. The icebergs, and any included debris, then drift under the action of ocean currents and, to a lesser extent, wind. The icebergs melt and fragment during their drift. As they melt, at a rate dependent on the temperature of the water, and their size and velocity, any included sediment is released. Coarser material rains out to the sea floor directly, whereas silts and clays have a residence time in the water column linked to particle size, surface roughness and water viscosity. Those parts of an iceberg exposed above water also melt, and debris released there can build up on the surface to be deposited as a single event when the iceberg fragments or overturns. Icebergs vary in diameter from meters to tens and even over 100 km on initial calving, and can be hundreds of meters in thickness. They may travel up to several thousand kilometers from their glacier source before complete melting, providing a mechanism of long-distance transport for included debris.

Sea ice forms during winter as the sea-surface freezes. Its drift is controlled mainly by wind because, at only a few meters in thickness but covering millions of square kilometers of the ocean, wind shear on its surface is particularly important. Sea ice melts from its base as it drifts into warmer waters, and at its surface due to increased radiative energy in summer. Predominantly fine-grained sediments are released in this way, in contrast to the delivery of material of heterogeneous grain size from icebergs.

Sedimentology of IRD

Deep-ocean sediments are usually fine-grained muds or oozes that are deposited in an environment of low energy. Floating ice, mainly in the form of icebergs, is the only mechanism by which significant quantities of very coarse-grained debris can be delivered into such environments. Individual pebbles, sometimes referred to as dropstones or lonestones, within fine-grained massive muds are a clear indicator of IRD deposition. Often dropstones exhibit striated and faceted surfaces, confirming their glacial origin. In higher energy marine environments, closer to the glacier source of icebergs and meltwater, isolated pebbles can be found within laminated silts and clays. Sometimes the laminations beneath the pebble have been deformed downward by the clast, and overlying sediments are, in turn, draped over it. Where large numbers of icebergs have traversed an area, releasing debris on melt or overturn, layers of sandy material have been observed, known as ice-rafted debris layers (Bond et al., 1992).

Paleoenvironmental significance

At timescales of hundreds of millions of years, the occurrence of isolated dropstones has been used to provide evidence of past ice ages, during which sufficient ice built up on land to reach the sea and produce sediment-laden icebergs. The occurrence of six ice ages over the past thousand million years of Earth history has been inferred using this and other evidence (Eyles, 1993). The first occurrence of IRD in long cores from the Late Cenozoic geological record has also been used to identify the initial growth of ice sheets on Antarctica and Northern Hemisphere landmasses.

The record of IRD deposition is usually constructed by counting the numbers of grains larger than a given size, often between 0.5 and 2 mm, per increment of core depth. Cores spanning the last glacial-interglacial cycle of about 115,000 years have also been examined at high resolution. The most easily distinguished ice-rafted layers yet found are the six so-called "Heinrich Layers," deposited as six events in North Atlantic cores over the past 60,000 years or so (Heinrich, 1988; Bond et al., 1992). Each IRD layer represents a collapse of the Hudson Bay-Hudson Strait drainage basin of the North American Ice Sheet, with the discharge of huge numbers of icebergs into the North Atlantic. The thickness of these Heinrich Layers decreases from about 0.5 m offshore of eastern Canada, to just a few centimeters some 3,000 km away off western Europe (Dowdeswell et al., 1995). Other IRD layers, less thick and continuous over space, probably indicate instabilities within smaller ice-sheet drainage basins, and have also been used to infer regional climatic and sea-level changes. However, IRD

layers are sometimes difficult to correlate over large distances because the very nature of iceberg drift and fragmentation is statistical, and long-distance correlations of IRD layers may be restricted to the products of major ice-sheet collapse events (Dowdeswell et al., 1999).

Finally, the sources and drift tracks of icebergs can be reconstructed from the mineralogical analysis of IRD grains. Debris derived from characteristic source rocks can be identified several thousands of kilometers distant, allowing patterns of past ocean currents to be reconstructed. The work of Bischof (2001) on the sources and drift tracks of icebergs in the Arctic Ocean provides an example of the use of mineralogical tracers.

Julian A. Dowdeswell

Bibliography

Anderson, J.B., Domack, E.W., and Kurtz, D.D., 1980. Observations of sediment-laden icebergs in Antarctic waters: Implications to glacial erosion and transport. *J. Glaciol.*, **25**, 387–396.

Barnes, P.W., Reimnitz, E., and Fox, D., 1982. Ice rafting of fine-grained sediment, a sorting and transport mechanism, Beaufort Sea, Alaska. *J. Sediment. Petrol.*, **52**, 493–502.

Bischof, J., 2001. *Ice Drift, Ocean Circulation and Climate Change.* Heidelberg: Springer.

Bond, G., Heinrich, H., Broecker, W., Labeyrie, L., McManus, J., Andrews, J., Huon, S., Jantschik, R., Clasen, S., Simiet, C., Tedesco, K., Klas, M., Bonani, G., and Ivy, S., 1992. Evidence for massive discharges of icebergs into the North Atlantic during the last glacial period. *Nature*, **360**, 245–249.

Dowdeswell, J.A., 1986. The distribution and character of sediments in a tidewater glacier, southern Baffin Island, N.W.T., Canada. *Arctic Alpine Res.*, **18**, 45–56.

Dowdeswell, J.A., Maslin, M.A., Andrews, J.T., and McCave, I.N., 1995. Iceberg production, debris rafting, and the extent and thickness of Heinrich layers (H-1, H-2) in North Atlantic sediments. *Geology*, **23**, 301–304.

Dowdeswell, J.A., Elverhøi, A., Andrews, J.T., and Hebbeln, D., 1999. Asynchronous deposition of ice-rafted layers in the Nordic seas and North Atlantic Ocean. *Nature*, **400**, 348–351.

Eyles, N., 1993. Earth's glacial record and its tectonic setting. *Earth Sci. Rev.*, **35**, 1–248.

Heinrich, H., 1988. Origin and consequences of cyclic ice rafting in the north-east Atlantic during the past 130,000 years. *Quaternary Res.*, **29**, 143–152.

Nürnberg, D., Wollenburg, I., Dethleff, D., Eicken, H., Kassens, H., Letzig, T., Reimnitz, E., and Thiede, J., 1994. Sediments in Arctic sea ice: Implications for entrainment, transport and release. *Mar. Geol.*, **119**, 185–214.

Cross-references

Binge-Purge Cycles of Ice Sheet Dynamics
Diamicton
Glaciomarine Sediments
Heinrich Events

INTEGRATED OCEAN DRILLING PROGRAM (IODP)

Introduction

Studies of the ocean floor have greatly improved our understanding of processes responsible for the evolution of oceans and continents. Because the geology of oceans is simpler than that of continents and because the oceans are relatively young, reconstruction of their geologic history is simpler. However, the oceans hide crustal rocks under sediment cover that can be several kilometers thick. We can study the underlying rocks by remote-sensing geophysical means and geochemical analyses of rocks recovered by coring and dredging. Definitive knowledge about the composition of underlying rocks and the processes responsible for their formation can only be obtained by acquiring samples, and that can only be accomplished by drilling and coring operations. It is not surprising, therefore, that scientific deep-ocean drilling, which started in 1968, has greatly increased our knowledge about the Earth. The Integrated Ocean Drilling Program is a complex international scientific drilling program that currently operates throughout the world.

Legacy programs

Scientific deep-ocean drilling started in 1968 with the Deep Sea Drilling Project (DSDP). The project's drillship was the *GLOMAR CHALLENGER,* whose operations were managed by the Scripps Institution of Oceanography. The drillship succeeded in overcoming several technical challenges, including dynamic positioning (how to keep the drillship positioned over the borehole in the presence of currents) and heave compensation (how to compensate for the ship's heave, so that the cores represent proper vertical positioning of the rock layers). DSDP's spectacular achievements became evident through the wealth of scientific results that emerged after drilling and coring at more than 600 sites throughout the world's oceans – all oceans except the Arctic. The DSDP verified seafloor spreading in the South Atlantic – ages were determined from examination of marine magnetic anomalies and were confirmed radiometrically, by comparing age from basement core samples. By obtaining core samples in all the oceans and by correlating the layering in the samples to environmental conditions, the field of paleoceanography was launched. Before DSDP started, a large number of seismic reflection profiles had been obtained in the world's oceans. Drilling, however, established the identity of layering in the seismic reflection profiles.

DSDP was succeeded by the Ocean Drilling Project (ODP) in 1985. The *JOIDES RESOLUTION* was the drillship used and the project was run by Texas A&M University. This program continued until 2003 and involved drilling at more than 650 sites. As more and more complex targets were attempted, technical innovations became necessary and a number of scientific discoveries were made. Among these were the presence of extensive microbial populations and the recovery of frozen methane reservoirs beneath the deep seafloor. It became possible to investigate fluid flow in the crust in several environments. The presence of vast sand deposits in deep water was discovered. Much was learned about the evolution of continental margins and new investigations probed the enigmatic large igneous provinces in the oceans.

Some of the major paleoclimate discoveries made under DSDP and ODP include:

- *Development of the field of paleoceanography.* The near-global network of continuous stratigraphic sections obtained by ocean drilling is the foundation of the field of paleoceanography.
- *Orbital variability during the Cenozoic.* By linking the record of climatic variation preserved in deep-sea sediments to calculated variations in Earth's orbital parameters, scientists have demonstrated the role of orbital variability in driving climate change.

- *Development of high-resolution chronology.* Complete recovery of fossiliferous marine sedimentary sections has greatly facilitated linking Earth's geomagnetic polarity reversal history to evolutionary biotic changes and to the isotopic composition of the global ocean.
- *Ocean circulation changes on decadal to millennial timescales.* The record preserved in marine sediments and recovered by ocean drilling has clearly demonstrated that deep- and surface-ocean circulation is variable on decadal to millennial timescales, confirming results from polar ice cores.
- *Global oceanic anoxic events.* Deep-sea sediments exhibit specific times when the surface water productivity of large areas of the ocean was unusually high.
- *Timing of ice-sheet development in Antarctica and the Arctic.* Drilling has revealed that Earth's entry into its current Ice Age extended over 50 Myr.
- *Sea-level change and global ice volume.* Marine sediments recovered from shallow water areas have shown that important global sea-level changes have occurred synchronously through at least the past 25 Myr, and that these changes can be matched to oxygen isotope records of climate produced from the deep sea.
- *Uplift of the Himalayas and the Tibetan Plateau.* Drilling results have shown that the onset and development of both the Indian and Asian monsoons are the result of climate change associated with this uplift.

The Initial Science Plan for IODP

The success of DSDP and ODP encouraged scientists interested in scientific drilling to inquire whether a new program could be launched aimed at previously unreachable drilling targets. Some of these targets were located beneath the ice-covered Arctic Ocean. Others involved drilling to great depths, where the stability of the borehole could not be assured with existing techniques, or where the release of hydrocarbon fluids under pressure could lead to blow-outs. A number of international conferences were held based on the premise that the drilling program needed enhancements – new drilling platforms were needed that could deal with problems associated with stability of drill hotels, with blow-out prevention, and with difficult locations such as ice-covered seas and shallow water depths (where the *JOIDES RESOLUTION* could not be used). These conferences included the Conference on Cooperative Ocean Riser Drilling (CONCORD) in Tokyo (1997), the Conference on Multiple Platform Exploration of the Ocean (COMPLEX) in Vancouver (1999), and a workshop on Alternate Drilling Platforms (APLACON) in Brussels (2001), as well as several other workshops and conferences. The conclusions from these meetings formed the basis of deliberations by an Integrated Ocean Drilling Program (IODP) Planning Subcommittee (IPSC), which provided a report entitled "Earth, Oceans, and Life." The report outlines the IODP Initial Science Plan for 2003–2013 and constitutes the program's scientific basis. It outlines three principal scientific themes and eight new initiatives derived from these themes, as well as principles of implementation.

The principal themes include *the deep biosphere and the subseafloor ocean*; *environmental change*, *processes*, *and effects*; and *solid Earth cycle and geodynamics*.

Within the science plan themes, the following initiatives are detailed:

- *Deep biosphere*

"Define bounding temperatures, pH and redox potential of the subseafloor biosphere ecosystem."

"Evaluate the biogeochemical impacts of the subseafloor microbiota."

"Provide uncontaminated samples necessary for high priority studies of deep-biospheric trophic strategies."

- *Gas hydrates*

"Explore the nature of gas hydrates and the range of depositional settings; study the origin of the gas and the processes of its migration and entrapment."

- *Extreme climates*

"Understand the mechanisms by which climate extremes develop and are maintained."

Understanding the mechanisms by which climactic extremes develop, are maintained and end is fundamental to a quantitative description of global change. Earth is now in one of those extremes, the geologically unusual situation of bipolar glaciation. Our knowledge of how Earth's system operates to maintain the current climate is relatively good, but we are still debating how the climate has reached this state.

A question of fundamental importance is how, once established, Earth's climate system operated to maintain the low thermal gradients indicated by warm, high-latitude climates. The paradox in this case is the apparent requirement to transport the great amount of heat needed to warm the poles, versus the sluggish oceanic and atmospheric circulation suggested by low pole-to-equator thermal gradients.

- *Rapid climate change*

"Recover detailed marine sedimentary records to examine the presence of rapid climate changes in the past."

One of the most striking results of recent paleoclimate research has been the determination that climate can change abruptly across the globe. For example, during the last glacial cycles, jumps between warmer and colder states occurred within decades, and these jumps were often associated with alternations in ocean circulation patterns.

Records of "natural" rapid climate change provide an indispensable context for evaluating contemporary anthropogenic inputs to the environment. The timing and distribution of the present warming trend may match those of previous times, or they may differ in some way explainable only by anthropogenic forcing. Such comparisons are greatly facilitated by recovery and use of detailed marine sedimentary records with resolutions approaching those of instrumental records.

The Arctic Ocean is essentially unknown, yet has the potential to advance our knowledge of rapid climate change processes enormously.

- *Continental break-up and sedimentary basin formation*

"Investigate difference in continental break-up and sediment basin formation at volcanic and non-volcanic margins."

- *Large igneous provinces*

"Understand mantle behavior during the massive episodic magmatic events that are responsible for the formation of large igneous provinces and determine potential causal relationships and feedback mechanisms between their formation and environmental change."

- *Twenty-First Century Mohole*

"Recover a complete section of oceanic crust and uppermost mantle and advance significantly our understanding

of the processes governing the formation and evolution of oceanic crust."

- *Seismogenic zone*

"Understand the nature of the seismogenic zone and mechanics of the earthquake cycle through a comprehensive, multidisciplinary project focused on the behavior of rocks, sediments and fluids in the fault zone region."

The above initiatives give a flavor of IODP plans. IODP is to be dynamic in nature and further initiatives will result as drilling proceeds.

Certain principles have been agreed on during IODP's implementation. Foremost is the coordinated use of multiple drilling platforms. (The individual drilling platforms will be discussed in the next section.) A comprehensive engineering development program will be developed to provide a number of special measurement and sampling tools. Existing logging programs will be reviewed and enhanced as necessary. Boreholes drilled as part of IODP will be instrumented to serve as sub ocean-bottom observatories. These initiatives will require coordination with other scientific programs that demonstrate interest in such observatories. For example, coordination and cooperation with programs involved in climate change may be desirable, as well as with industry, which shares similar goals with IODP.

Drilling ships and platforms

Scientists participating in the IODP will be able to make use of three drilling platforms:

- The riser-equipped drilling vessel, the *CHIKYU*, built by JAMSTEC (acronym for the Japan Agency for Marine-Earth Science and Technology);
- A riserless platform provided by the United States, the *JOIDES RESOLUTION*, a 143-m long drillship used in ODP and for the first phase of IODP operations has recently undergone major renovations.
- Mission-specific platforms contributed by European countries that can operate in ice-covered oceans, shallow water zones, and areas inaccessible to the drilling vessels *CHIKYU* and *JOIDES RESOLUTION*.

The centerpiece of IODP is the drilling vessel *CHIKYU*. Built at a cost of more than $500 million, the ship is 210 m long, and has a gross tonnage of 57,500 tons. The top of her 70-m derrick rises 116 m above the waterline. A dynamic positioning system can keep her within a 15-m radius above a drill hole. The *CHIKYU* contains a number of laboratories for intensive, non-destructive core analysis. These include a microbiology laboratory, a paleomagnetism laboratory, and a laboratory that includes an X-Ray CT scanner. It can drill 7 km beneath the ocean floor and can thus penetrate oceanic crust and reach the mantle. Drilling at a water depth of 2.5 km, the *CHIKYU* can wield a total drill pipe length of 9.5 km. Other distinguishing features of the *CHIKYU* include the availability of a riser and a blow-out preventer. The riser consists of a large diameter pipe which connects the drillship to the wellhead on the ocean floor and contains the drill pipe. Drilling fluid, which consists of "drilling mud," is pumped down through the drill pipe together with the cuttings (ground up bits of rock), and returns through the space between the drill pipe and the riser pipe to the drillship. The cuttings are separated by filtering, and the drilling fluid is recycled. Circulating the drilling mud through the riser pipe provides several advantages. Drilling mud is superior to seawater (which has to be used if there is no return circulation) in flushing the cuttings out, which otherwise could clog the drill hole. Appropriately dense mud can be used to line the drill hole and prevent it from caving in. In the absence of coring, the cuttings provide information about the formation that is being drilled through. When a riser is being used, a blow-out preventer sits over the drill hole. It acts as an automated shut-off device which provides protection against unintentional release of high pressure fluids and gases. The *CHIKYU* uses a massive 380-ton blow-out preventer, which contains a pressure-control system that maintains pressure at 15,000 pounds per square inch.

Mission-specific platforms are chosen for each mission-specific expedition. The Arctic Coring Expedition (ACEX) included a fleet of three icebreaker-class ships: a drilling vessel, the *VIDAR VIKING*, which remained at a fixed location and suspended more than 1,600 m of drill pipe through the water column and into the underlying sediments; a Russian nuclear icebreaker, the *SOVETSKIY SOYUZ*; and a diesel-electric icebreaker, the *ODEN*. The *SOVETSKIY SOYUZ* and *ODEN* protected the *VIDAR VIKING* by breaking "upstream" floes into smallish iceberg bits that allowed the *VIDAR VIKING* to stay positioned and recover sediment cores.

IODP structure

The IODP organization is complex. It includes Funding Agencies; Implementing Organizations, which run the drillships; the Science Advisory Structure, which provides scientific advice; and a Central Management Organization. The two Lead Funding Agencies are the U.S. National Science Foundation (NSF) and the Japanese Ministry of Education, Culture, Sports, Science and Technology (MEXT). They provide equal funds for the program. Funds also are contributed by the European Consortium for Ocean Research Drilling (ECORD), which consists of 17-member countries. China's Ministry of Science and Technology (MOST) is an associate funding agency. The Implementing Organizations (IOs) include: the USIO comprising the Consortium for Ocean Leadership, Texas A&M University, and Lamont-Doherty Earth Observatory – the USIO operates the *JOIDES RESOLUTION*; CDEX, the Center for Deep Earth Exploration, part of JAMSTEC, operates the *CHIKYU*; and ESO, the European Consortium for Research Drilling (ECORD) Science Operator, which operates mission-specific platforms. The Science Advisory Structure (SAS) includes a number of committees and panels that provide scientific advice. Several hundred scientists serve on these committees and panels. IODP Management International (IODP-MI), a nonprofit corporation, serves as the Central Management Organization.

The structure of IODP can be perceived as a matrix with international funding agencies as program sponsors along one axis, and the Science Advisory Structure and Implementing Organizations along another axis, with the Central Management Office providing program focus.

Expeditions

IODP's first two expeditions (in 2004) were the Juan de Fuca Hydrogeology Expedition and ACEX. IODP's inaugural voyage was conducted at the Juan de Fuca Ridge in the summer of 2004, 200 km off the coast of British Columbia. Its objective was to conduct a series of studies to evaluate how fluid flows within oceanic crust. To succeed, the science party had to establish three "borehole observatories." Two new observatories were

installed nearly 600 m below the seafloor, and another was established to replace an existing observatory. When completed within the next few years, the observatory network will enable scientists to discern the flow pattern in the oceanic crust. Expedition 301, the Juan de Fuca, also sampled sediments, basalt, fluids and microbial samples, and collected wireline logs in the deepest borehole.

The Arctic Coring Expedition, the first scientific drilling expedition to the central Arctic Ocean followed, in late summer 2004. Expedition 302 recovered sediment cores deeper than 400 m below seafloor in water depths of ~1,300 m at a location only 250 km from the North Pole.

ACEX's destination was the Lomonosov Ridge, hypothesized to be a sliver of continental crust that broke away from the Eurasian Plate at ~56 Ma. As the ridge moved north and then subsided, marine sedimentation occurred and continued to the present, resulting in what was anticipated (from seismic data) to be a continuous paleoceanographic record. The elevation of the ridge above the surrounding abyssal plains (~3 km) ensures that sediments atop the ridge are free of turbidites. ACEX's primary scientific objective was to continuously recover this sediment record and sample the underlying sedimentary bedrock by drilling and coring from a stationary drillship.

ACEX's biggest challenge was maintaining the drillship's location while drilling and coring 2–4-m thick sea ice that moved at speeds approaching half a knot. Sea-ice cover over the Lomonosov Ridge moves with the Transpolar Drift and responds locally to wind, tides, and currents. Never before had the high Arctic Ocean Basin (known as "mare incognitum" within the scientific community) been deeply cored, primarily because of these challenging sea-ice conditions.

Initial offshore results, based on analysis of core catcher sediments, demonstrated that biogenic carbonate only occurs in the Holocene-Pleistocene interval. The upper ~170 m represent a record of the past ~15 Myr composed of sediment with ice-rafted sediment and occasional small pebbles, suggesting that ice-covered conditions extended at least this far back in time. Earlier in the record, spanning a major portion of the Oligocene to late Eocene, an interruption in continuous sedimentation occurred. This may represent a hiatus encompassing a time interval of non-deposition or an erosional episode that removed sediment of this age from the ridge. The sediment record during the middle Eocene is of dark, organic-rich siliceous composition. Isolated pebbles, interpreted as ice-rafted dropstones, are present well into the middle Eocene section. An interval recovered around the lower/middle Eocene boundary contains an abundance of *Azolla* spp., suggesting that a fresh/low-salinity surface-water setting dominated the region during this time period. Drilling revealed that, during the latest Paleocene to the earliest Eocene boundary interval known as the Early Eocene Thermal Maximum (EETM) or the Paleocene-Eocene Thermal Maximum (PETM), the Arctic Ocean was subtropical with warm surface-ocean temperatures. ACEX penetrated into the underlying sedimentary bedrock, revealing a shallow-water depositional environment of Late Cretaceous age.

IODP expeditions aboard the *JOIDES RESOLUTION* continued through 2005 into 2006. As of July 2005, six riserless expeditions were completed. Of the six, five occurred in the North Atlantic; the sixth was conducted in the deep Gulf of Mexico. The *JOIDES RESOLUTION* proceeded to the Pacific for the remainder of 2005 and a portion of 2006.

Two mission-specific operations, the Tahiti Sea Level and the New Jersey Sea Level Expeditions, were planned for implementation by ESO.

Brief descriptions of 2004–2005 IODP expeditions follow.

North Atlantic Climate

The objective of these two back-to-back expeditions was to establish the intercalibration of geomagnetic paleointensity, isotope stratigraphy, and regional environmental stratigraphies for the Late Neogene to Quaternary period, and to develop a millennial-scale stratigraphic template for the North Atlantic. Other objectives were: (a) to better understand the relative phasing of atmospheric, cryospheric, and oceanic changes central to the mechanisms of global climate change on orbital or millennial timescales; and (b) to improve our knowledge of the temporal and spatial behavior of the geomagnetic field through high-resolution records of directional secular variation and geomagnetic paleointensity. A total of 36 holes was drilled at 11 sites, and 6,998 m of core were retrieved from beneath the seafloor.

Complete sedimentary sections were drilled by multiple advanced piston coring directly south of the Central Atlantic "ice-rafted debris belt" and on the southern Gardar Drift. In addition to the North Atlantic paleoceanography study, a borehole observatory was successfully installed in a new 170 m deep hole close to an earlier Ocean Drilling Program site.

Core Complex

This two-expedition program was aimed at documenting the conditions under which oceanic core complexes (OCCs) develop. These large shallow seafloor features appear to be related to rifting and accretion at slow-spreading mid-ocean ridges. However, currently available data are inadequate to characterize the magmatic/tectonic/metamorphic history, which is needed to better understand the mechanisms of OCC uplift and emplacement. Two sites were drilled: a deep-penetration site on the central dome of Atlantis Massif to sample the detachment fault zone and the alternation front and to drill into unaltered mantle (core and logging analyses were planned); and a shallower-penetration site through the hanging wall to sample rock just above the detachment, the shallowest part of the unexposed fault, and through the fault zone (core and logging analyses were planned). Twenty-two holes were drilled at four sites, with a total of 1,113 m of core retrieved. Unfortunately, the unaltered mantle was not reached.

Porcupine Basin Carbonate Mounds

The Porcupine Basin Carbonate Mounds Expedition included drilling a downslope suite of three sites on the eastern slope of Porcupine Sea Bight, west of Ireland. The sites are centered on "Challenger mound," a 170-m high, partly buried carbonate mound in the "Belgica mound province," topped by dead, cold-water coral rubble. The Belgica mound province belongs to one of the world's most well-documented carbonate mound provinces. The on-mound site was expected to unveil the environmental record locked in a carbonate mound and to shed light on the processes which may have controlled the genesis of the mound – in particular to test the hypothesis of the possible role of fluid venting as a trigger for mound growth and to assess the importance of environmental forcing factors. Particular attention was paid to microbiological and biogeochemical processes in mound genesis and development.

Deepwater Gulf of Mexico

This expedition was named "Overpressure and Fluid Flow Processes in the Deepwater Gulf of Mexico: Slope Stability, Seeps,

and Shallow Water Flow." It was designed to explore the relationships that exist among and between overpressure, flow, and deformation in passive margin settings, and to test a multi-dimensional flow model by examining how physical properties, pressure, temperature, and pore fluid composition vary within low-permeability mudstones that overlie a permeable and over-pressured aquifer.

Superfast Spreading Crust

Two expeditions to examine the superfast spreading crust returned to an earlier ODP borehole to recover a complete section through >200 m yr^{-1} oceanic crust. Multiple trips to the drill sites resulted in retrieval of gabbros from intact ocean crust. In addition, for the first time, Scientists were able to drill through the entire sequence of volcanic rocks that cap the ocean crust to reach a fossil magma chamber 1.4 km beneath the seafloor. A complete section of the upper oceanic crust, drilled 1005 meters into the basement, was recovered.

Tahiti Sea Level

This expedition drilled a series of boreholes along a number of transects to: (a) reconstruct the deglaciation curve for the period 20,000–10,000 yBP in order to establish the minimum sea-level during the Last Glacial Maximum (LGM), and to assess the validity, timing and amplitude of meltwater pulses (so-called MWP-1A and MWP-1B events; ca. 13,800 and 11,300 cal. yBP), which are thought to have disturbed the general thermohaline oceanic circulation and, hence, global climate; (b) establish the sea surface temperature (SST) variation accompanying the transgression at each transect. These data will allow the examination of the impact of sea-level changes on reef growth, geometry and biological makeup, especially during reef drowning events, and will help improve the modeling of reef development; and (c) identify and establish patterns of short-term paleoclimatic changes that are thought to have punctuated the transitional period between present-day climatic conditions following the LGM. It is proposed to quantify the variations of sea surface temperatures based on high-resolution isotopic and trace element analyses on massive coral colonies. A attempt was made to identify specific climatic phenomena such as El Niño-Southern Oscillation (ENSO) in the time frame prior to 10,000 yBP.

Cascadia Margin Gas Hydrates

The Cascadia Margin Gas Hydrates proposal, designed in an accretionary prism environment, aimed to better constrain the models concerning the formulation of gas hydrates. Expedition 311 drilled a series of sites across the northern Cascadia accretionary prism to improve understanding of the deep origin of methane, its upward transport, its incorporation in gas hydrate, and its subsequent loss to the seafloor.

New Jersey Sea Level

This IODP expedition is to obtain continuous cores and downhole logging measurements of siliciclastic sequences from this modern continental margin within crucial paleo-inner-shelf facies at three sites that represent the most sensitive and accessible locations for deciphering amplitudes and testing facies models.

Conclusion

While surface samples in the ocean bottom can be recovered by coring and dredging, samples of deep rocks can only be recovered by deep drilling and coring. The deep drilling programs DSDP, ODP, and now IODP are programs that obtain rocks at great depths by coring and are therefore, by examination of these rocks, able to tell us much of climate conditions and ocean conditions at the time that the sediments that constitute the rocks were laid down. The science of paleoceanography can thus be said to have developed largely as a result of these drilling programs. Climate changes with frequencies ranging from several hundreds of thousands of years to the millennial scale have thus been elaborated through an examination of the cored rocks. The goals of IODP with respect to paleoceanography are focused on a number of specific problems; these include the studies of rapid climate change, as well as extreme climates and the variables that relate oceans to climate. During the next five years we expect major discoveries with respect to climates and oceans of the past, which in turn may give us clues as to what we can expect of climate and oceans in the future.

Manik Talwani

Bibliography

Farrell, J.W., and Prell, W.L., 1989. Climatic change and $CaCO_3$ preservation: An 800,000-year bathymetric reconstruction from the central equatorial Pacific. *Paleoceanography*, **4**, 447–466.

Hays, J.D., Imbrie, J., and Shackleton, N.J., 1976. Variations in Earth's orbit: Pacemaker of ice ages. *Science*, **194**, 1121–1132.

Kennett, J.P., 1977. Cenozoic evolution of Antarctic glaciation, the circum-Antarctic Ocean, and their impact on global paleoceanography. *J. Geophys. Res.*, **82**, 3843–3860.

Raymo, M.E., and Ruddiman, W.F., 1992. Tectonic forcing of late Cenozoic climate. *Nature*, **359**, 117–122.

Schrag, D.P., Hampt, G., Murray, D.W., 1996. The temperature and oxygen isotopic composition of the glacial ocean. *Science*, **272**, 1930–1932.

Zachos, J.C., Pagani, M., Sloan, L., Thomas, E., and Billups, K., 2001. Trends, rhythms, and aberrations in global climate 65 Ma to Present. *Science*, **292**, 686.

Cross-references

Deep Sea Drilling Project (DSDP)
Methane Hydrates, Carbon Cycling, and Environmental Change
Ocean Drilling Program (ODP)
Paleocene-Eocene Thermal Maximum
Paleoceanography

INTERSTADIALS

Definitions

Interstadials are regarded as the relatively short-lived periods of thermal improvement during a glacial phase, when temperatures did not reach those of the present day and, in lowland mid-latitude regions, the climax vegetation was boreal woodland (Lowe and Walker, 1997). Jessen and Milthers (1928) defined interstadials as periods that are either too short or too cold to allow the development of temperate deciduous forest of interglacial type in the same region. Interstadials are, however, not only defined on biostratigraphical grounds. In the USA, for instance, an interstadial is formally regarded as a climatic episode within a glaciation during which a secondary recession or standstill of glaciers took place (Gibbard and West, 2000).

Table I4 Interstadials during the Weichselian in Europe: Denmark (*DK*), The Netherlands (*NL*), Germany (*D*) France (*F*), Great Britain (*UK*), compared to GRIP Summit glacial interstadials IS as defined by Dansgaard et al. (1993)

Terrestrial sequences Europe	IS
Bølling-Allerød (DK), Windermere (UK)	1
Denekamp (NL)	8
Hengelo (NL)	12
Moershoofd (NL)	13
Glinde (D)	14
Oerel (D)	16
Odderade (D) St. Germain II (F)	21
Brørup (DK), St. Germain I (F), Chelford (UK)	23
Amersfoort (NL)	

Interstadials during the Weichselian

Many different interstadials are defined in Europe based on palynology. The interstadials that occurred during, for instance, the Weichselian Glacial have been named after the place where the interstadial was described for the first time. Many of these Weichselian interstadial stratotypes have been defined in NW Europe and are described by Behre (1989), Zagwijn (1989), and de Beaulieu and Reille (1992) (Table I4). Dansgaard et al. (1993) described 24 interstadial phases in the GRIP oxygen isotope record from the Greenland ice, characterized by a sudden increase and gradually decrease of oxygen isotope values. Recent evidence points to a total of 25 interstadial phases that are resolved in the Greenland ice core (NGRIP Members, 2004). These so-called Dansgaard-Oeschger interstadial events can be correlated with low percentages of the planktonic cold water foraminifera *Neogloboquadrina pachyderma* in high-resolution records from the North Atlantic (Bond et al., 1993).

Wim Z. Hoek

Bibliography

Behre, K.E., 1989. Biostratigraphy of the last glacial period in Europe. *Quaternary Sci. Rev.*, **8**, 25–44.

Bond, G., Broecker, W., Johnsen, S., McManus, J., Labeyrie, L., Jouzel, J., and Bonani, G., 1993. Correlations between climate records from North Atlantic sediments and Greenland ice. *Nature*, **365**, 143–147.

Dansgaard, W., Johnsen, S.J., Clausen, H.B., Dahl-Jensen, D., Gundestrup, N.S., Hammer, C.U., Hvidberg, C.S., Steffensen, J.P., Sveinbjörnsdottir, A.E., Jouzel, J., and Bond, G., 1993. Evidence for general instability of past climate from a 250-kyr ice-core record. *Nature*, **364**, 218–220.

de Beaulieu, J.L., and Reille, M., 1992. The last climatic cycle at La Grande Pile (Vosges, France): A new pollen profile. *Quaternary Science Reviews*, **11**, 431–438.

Jessen, K., and Milthers, V., 1928. Stratigraphical and palaeontological studies of interglacial freshwater deposits in Jutland and north-west Germany. *Danmarks Geologiske Undersøgelse II*, **48**, 380pp.

Gibbard, P.L., and West, R.G., 2000. Quaternary chronostratigraphy: The nomenclature of terrestrial sequences. *Boreas*, **29**, 329–336.

Lowe, J.J., and Walker, M.J.C., 1997. *Reconstructing Quaternary Environments.* London, UK: Longman, 446pp.

North Greenland Ice Core Project (NGRIP) Members, 2004. High-resolution record of Northern Hemisphere climate extending into the last interglacial period. Nature, **431**, 147–151.

Zagwijn, W.H., 1989. Vegetation and climate during warmer intervals in the Late Pleistocene of western and central Europe. *Quaternary Int.*, **3–4**, 57–67.

Cross-references

Bølling-Allerød Interstadial
Millennial Climate Variability
Dansgaard-Oeschger Cycles
Ice Cores, Antarctica and Greenland
Oxygen Isotopes
Palynology
Pollen Analysis

IRON AND CLIMATE CHANGE

Iron availability limits the ability of phytoplankton in some parts of the surface ocean to photosynthesize biomass from dissolved CO_2 in seawater. An important source of iron to phytoplankton is the deposition of dust from continents. The sensitivity of dust deposition to climatic factors such as aridity and windiness makes iron a possible link between climate and the CO_2 concentration in the atmosphere. Iron climate linkages and their biogeochemical ramifications are explored further in a recent article by Jickels et al. (2005).

The element iron is abundant in the core and crust of the Earth. In the early Earth, the oceans contained high concentrations of dissolved iron in the form of Fe^{2+}. However, as the oceans became oxidized by increasing O_2 concentrations in the atmosphere, iron oxidized to the relatively insoluble state Fe^{3+}, and deposited into sedimentary structures known as Banded Iron Formations. Except for anoxic regions such as in sediments or isolated basins such as the Black Sea, dissolved iron concentrations have remained low in the oceans ever since.

However, iron is not absent in the oxic ocean. Fe^{3+} is stabilized in the dissolved form by complexing organic compounds called chelators or siderophores (Rue and Bruland, 1995). These compounds appear to be biogenic, but little is known of their structure, lifetime, or origins. Similar compounds are secreted in soil and freshwater systems to enable plants, fungi, and bacteria to acquire iron. A vast majority of the iron in seawater is found to be complexed to siderophores. In addition, the precipitation of Fe^{3+} into solid form does not result in its immediate removal by sinking when the particles generated are very small. More than half of the Fe^{3+} in seawater is found in colloidal form, too small to sink but potentially too large to be biologically useful. In particular, the diffusion coefficient of colloidal complexed iron will be slower than that for truly dissolved iron, and its availability for biological uptake will be correspondingly less (Wu et al., 2001).

In spite of its scarcity, iron is an essential co-factor in enzymatic systems such as the light-harvesting photosynthesis systems, and in nitrogenase, the enzyme which fixes NH_4^+ from molecular N_2 (Falkowski et al., 1998). Because of its low solubility in oxic seawater, iron has been shown to limit the production of biomass in several regions of the surface ocean. These regions, historically called High Nutrient Low Chlorophyll (HNLC) regions, include the equatorial Pacific, the North Pacific, and the Southern Ocean. When the iron concentration in the surface ocean is artificially increased in these areas, the iron stimulates increases in chlorophyll concentration, photosynthetic efficiency, and phytoplankton growth rates (Coale et al., 1996). These iron fertilization experiments constitute one of the most dramatic breakthroughs in biological oceanography in several decades.

The link between phytoplankton and the CO_2 concentration of the atmosphere occurs via the biological pump in the ocean. Photosynthesis produces particles that can leave their source waters by sinking. The downward net flux of biological material leaves the surface ocean depleted in nutrients such as NO_3^{2-} and PO_4^{3-}, as well as dissolved CO_2. CO_2 gas dissolves into surface seawater, or evaporates into the atmosphere, according to its concentration in seawater or air, and its solubility (mostly controlled by temperature). Depletion of CO_2 from surface waters by biological activity therefore draws down the CO_2 concentration of the atmosphere. In the present-day ocean, Southern Ocean surface waters contain the majority of the potentially biologically usable nutrients NO_3^{2-} and PO_4^{3-}. In addition, because the Southern Ocean is a conduit to the largest oceanic carbon reservoir – the deep ocean, atmospheric pCO_2 in models is more sensitive to surface chemistry changes in the Southern Ocean than other oceanographic regions. Therefore, the search for an explanation for lower glacial pCO_2 values has centered on deposition of iron onto the Southern Ocean.

There are arguments for and against the Southern Ocean fertilization hypothesis. On the positive side, the deposition of dust and Fe in Antarctic ice cores was indeed higher during glacial times, by more than an order of magnitude. Most of this dust appears to originate from a specific region in Patagonia, but dust deposition increased globally by a factor of two or more. The decline in Antarctic dust deposition is also one of the earliest indicators of the coming deglaciation (suggesting that dust decrease could be an ultimate cause for the other aspects of the deglaciation) (Broecker and Henderson, 1998).

On the other hand are arguments against the Southern Ocean fertilization hypothesis. Several models of iron geochemistry in the ocean conclude that the dominant iron source to the Southern Ocean surface is from below, in the upwelling water, and that increasing the negligible deposition flux will have little effect (Archer and Johnson, 2000). Fertilization experiments in the Southern Ocean have not resulted in increased sinking of organic matter into deep waters, but rather an increased standing biomass stock in surface waters as the added iron is efficiently recycled (Boyd et al., 2000). Trace element tracers for sea surface nutrient concentration in the Southern Ocean have not shown a substantial drawdown during glacial time (Boyle, 1992). Furthermore, the pCO_2 sensitivity to the Southern Ocean decreases with increasing model complexity and realism, such that even a complete drawdown of Southern Ocean nutrients would not be enough to generate glacial pCO_2 values (Archer et al., 2000). Finally, an increase in the biological pump would result in a decrease in the O_2 concentration of the deep ocean, which is not apparent in the sedimentary record.

With these counter-arguments in mind, the community is also investigating the possibility that an increased glacial iron supply might stimulate an increase in nitrogen fixation, resulting in an increase in the nitrate inventory of the ocean (Broecker and Henderson, 1998). A release from nitrogen limitation might result in a stronger biological pump, although phosphorus availability could limit this effect. In addition, iron fertilization is being explored as a potential fix for rising CO_2 concentrations resulting from fossil fuel consumption.

David Archer

Bibliography

Archer, D.E., and Johnson, K., 2000. A model of the iron cycle in the ocean. *Global Biogeochem. Cycles*, **14**, 269–279.

Archer, D., Eshel, G., Winguth, A., Broecker, W.S., Pierrehumbert, R.T., Tobis, M., and Jacob, R., 2000. Atmospheric pCO_2 sensitivity to the biological pump in the ocean. *Global Biogeochem. Cycles*, **14**, 1219–1230.

Boyd, P.W., Watson, A.J., Law, C.S., Abraham, E.R., Trull, T., Murdoch, R., Bakker, D.C.E., Bowie, A.R., Buesseler, K.O., Chang, H., Charette, M., Croot, P., Downing, K., Frew, R., Gall, M., Hadfield, M., Hall, J., Harvey, M., Jameson, G., LaRoche, J., Liddicoat, M., Ling, R., Maldonado, M.T., McKay, R.M., Nodder, S., Pickmere, S., Pridmore, R., Rintous, S., Safi, K., Sutton, P., Strzepek, R., Tannaberger, K., Turner, S., Waite, A., and Zeldis, J., 2000. A mesoscale phytoplankton bloom in the polar Southern Ocean stimulated by iron fertilization. *Nature*, **407**, 695–702.

Boyle, E.A., 1992. Cadmium and $\delta^{13}C$ paleochemical ocean distributions during the Stage 2 glacial maximum. *Annu. Rev. Earth Planet. Sci.*, **20**, 245–287.

Broecker, W.S., and Henderson, G., 1998. The sequence of event surrounding termination II and their implications for the cause of glacial-interglacial CO_2 changes. *Paleoceanography*, **13**, 352–364.

Coale, K.H., Johnson, K.S., Fitzwater, S.E., Gordon, R.M., Tanner, S., Chavez, F.P., Ferioli, L., Sakamoto, C., Rogers, P., Millero, F., Steinberg, P., Nightingale, P., Cooper, D., Cochlan, W.P., Landry, M. R., Constantinou, J., Rollwagen, G., Trasvina, A., and Kudela, R., 1996. A massive phytoplankton bloom induced by an ecosystem-scale iron fertilization experiment in the equatorial Pacific Ocean. *Nature*, **383**, 495–501.

Falkowski, P.G., Barber, R.T., and Smetacek, V., 1998. Biogeochemical controls and feedbacks on ocean primary production. *Science*, **281**, 200–206.

Jickels, T.D., 2005. Global iron connections between desert dust, ocean biogeochemistry, and climate. *Science*, **308**, 67–71.

Rue, E.L., and Bruland, K.W., 1995. Complexation of iron(III) by natural organic ligands in the Central North Pacific as determined by a new competitive ligand equilibration/absorptive cathodic stripping voltammetric method. *Mar. Chem.*, **50**, 117–138.

Wu, J., Boyle, E., Sunda, W., and Wen, L.-S., 2001. Soluble and colloidal iron in the oligotrophic North Atlantic and North Pacific. *Science*, **293**, 847–849.

Cross-references

Banded Iron Formations and the Early Atmosphere
Marine Carbon Geochemistry

ISOTOPE FRACTIONATION

Isotopes are atoms whose nuclei contain the same number of protons but a different number of neutrons. The term 'isotope' is derived from a Greek word meaning equal place: the various isotopes of an element occupy the same position in the periodic table. Isotopes of an element can be either stable or unstable (radiogenic). Differences in chemical and physical properties arising from variations in atomic mass of an element are called '*isotope effects*'. The partitioning of isotopes between two substances or two phases of the same substance with different proportions of isotopes is called '*isotope fractionation*' (Hoefs, 1997; Criss, 1999).

The isotopic composition of materials contains information that can be used, for example, to reconstruct the palaeoenvironment and to understand the hydrological cycle and biochemical pathways.

History

In 1913, isotopes were discovered by J. J. Thomson who found that the element neon has two different kinds of atoms with atomic weights 20 and 22. A few years later, 212 of the 287

naturally occurring isotopes were known. The reason for the existence of isotopes was, however, unclear until the discovery of the neutron by Chadwick in 1932. The seminal papers by Urey (1947) and Bigeleisen and Mayer (1947) on the thermodynamic properties of isotopic substances provided the basis for the utilization of stable isotopes in geology, geochemistry, biogeochemistry, paleoceanography and elsewhere.

Notation, definitions

Isotopic ratios, R, are measures of the relative abundances of isotopes of an element, E; they are usually arranged so that the lightest stable isotope (index a), which is often also the most abundant isotope, appears in the denominator: ${}^{b}R = {}^{b}\mathrm{E}/{}^{a}\mathrm{E}$ (stable boron isotopes are an exception: ^{11}B is about four times more abundant than ^{10}B). The three stable oxygen isotopes ^{16}O, ^{17}O, and ^{18}O will be used to explain the notation and basic definitions.

The oxygen isotope with mass number 16 contains 8 protons and 8 neutrons and is denoted by ^{16}O. It is by far the most abundant (99.76%) of the three stable oxygen isotopes. For example, the ratio of ^{17}O to ^{16}O in water, or the ratio of ^{18}O to ^{16}O in carbon dioxide can be written as:

$$ {}^{17}\mathrm{R}_{\mathrm{H_2O}} = \frac{[\mathrm{H_2}{}^{17}\mathrm{O}]}{[\mathrm{H_2}{}^{16}\mathrm{O}]}, \quad {}^{18}\mathrm{R}_{\mathrm{CO_2}} = \frac{2\,[\mathrm{C}{}^{18}\mathrm{O}{}^{18}\mathrm{O}] + [\mathrm{C}{}^{18}\mathrm{O}{}^{16}\mathrm{O}]}{2\,[\mathrm{C}{}^{16}\mathrm{O}{}^{16}\mathrm{O}] + [\mathrm{C}{}^{18}\mathrm{O}{}^{16}\mathrm{O}]} $$

The *isotopic composition*, δ, of a sample, determined by mass spectrometric methods, is measured with respect to a standard (std):

$$ \delta^{b}\mathrm{E}_{\mathrm{sample}} = \left(\frac{{}^{b}\mathrm{R}_{\mathrm{sample}}}{{}^{b}\mathrm{R}_{\mathrm{std}}} - 1 \right) \cdot 1{,}000 $$

where b is the atomic mass of the isotope and the factor 1,000 converts the δ value to per mil. The standards (cf. Hoefs, 1997) used for stable oxygen isotopes are V-SMOW (Vienna-Standard Mean Ocean Water; ${}^{18}R_{\mathrm{V\text{-}SMOW}} \cdot 10^{6} = 2{,}005.20 \pm 0.43$) and V-PDB (Vienna-Pee-Dee Belemnite, ${}^{18}R_{\mathrm{V\text{-}PDB}} \cdot 10^{6} = 2{,}067.1 \pm 2.1$).

The *fractionation factor*, α, is defined as the ratio between the isotopic ratio in compound X and that in compound Y:

$$ {}^{b}\alpha_{(\mathrm{X-Y})} = \frac{{}^{b}R_{\mathrm{X}}}{{}^{b}R_{\mathrm{Y}}} = \frac{\delta^{b}\mathrm{E_X} + 1{,}000}{\delta^{b}\mathrm{E_Y} + 1{,}000} $$

It is a measure of the partitioning of isotopes between two or more phases in response to an isotope effect.

Whereas the δ value is the result of the whole history of the sample, the α value is characteristic for, say, an equilibrium between X and Y or for a process that leads from X to Y. Since α values are usually very close to 1.0, the ε notation is commonly used to express isotope fractionations in per mil (±‰):

$$ {}^{b}\varepsilon_{(\mathrm{X-Y})} = \left({}^{b}\alpha_{(\mathrm{X-Y})} - 1\right) \cdot 1{,}000 $$

Isotope effects

The most important isotope effects arise from differences in: (a) random mean velocities and (b) vibrational frequencies of molecules.

a) Random mean velocity effects. In (local) thermodynamic equilibrium, the mean kinetic energy is equal for all molecules and determined by temperature alone:

$$ \left\langle \mathrm{E}_{\mathrm{kin},j} \right\rangle = \frac{1}{2} m_j \left\langle v_j{}^{2} \right\rangle = \frac{3}{2} k_B\, T = \mathrm{E}_{\mathrm{thermal}} $$

where m_j and $v_{\mathrm{rms},j} = \sqrt{\left\langle v_j^{2} \right\rangle}$

are mass and random mean square (rms) velocity of molecule j, k_{B} is Boltzmann's constant, and T is absolute temperature. At a given temperature, the rms velocity varies with the mass of the molecule: light molecules are faster than heavy molecules (Graham's law of diffusion):

$$ v_{\mathrm{rms},1} / v_{\mathrm{rms},2} = \sqrt{m_2 / m_1} $$

As a consequence, molecules containing the light isotope diffuse faster. The ratio of the diffusion coefficients D_v for the light (mass m_a) and the heavy molecule (mass m_b) of a gas that diffuses through air (mass $m_c = 29$) is given by

$$ \alpha_{(a-b)} = \frac{D_b}{D_a} = \sqrt{\frac{m_b + m_c}{m_b \cdot m_c} \frac{m_a \cdot m_c}{m_a + m_c}} $$

For $^{13}CO_2$ and $^{12}CO_2$, one obtains

$$ {}^{13}\alpha_{\mathrm{diff.\ CO_2\ in\ air}} = \sqrt{\frac{45 + 29}{45 \cdot 29} \frac{44 \cdot 29}{44 + 29}} \approx 0.9956 $$

The relation does not apply, however, for diffusion of gases through liquids where the ratio of the diffusion coefficients is closer to one (${}^{13}\alpha_{\mathrm{diff.\ CO_2\ in\ water}} \approx 0.9993$). The variation of the rms velocity with mass also leads to differences in evaporation.

b) Effects due to molecular vibrations. The zero-point energy of vibrations in molecules, E_0, is mass dependent. For diatomic molecules $E_0 = h\nu/2$, where h is Planck's constant and ν is the (vibration) frequency. The ratio of frequencies ν and ν' for two diatomic molecules of different isotopic composition is approximately given by $\nu'/\nu = (\mu/\mu')^{1/2}$ where $\mu = m_1 \cdot m_2/(m_1 + m_2)$ is the reduced mass and m_1 and m_2 are the masses of the two atoms involved.

Example: compare the frequencies for ^{16}O ^{16}O (ν, $\mu = 16 \cdot 16/(16 + 16) = 8$), ^{17}O ^{16}O ($\nu'$, $\mu' = 17 \cdot 16/(17 + 16) \approx 8.2424$), and ^{18}O ^{16}O ($\nu''$, $\mu'' = 18 \cdot 16/(18 + 16) \approx 8.4706$): $\nu'/\nu \approx 0.9852$, $\nu''/\nu \approx 0.9718$, i.e., the strength of the isotope effect increases with the mass difference and thus it is not surprising that the resulting isotope fractionation is also 'mass-dependent', as a rule.

Isotope fractionation

The difference in isotopic composition between various compounds or between various phases of a single compound is called isotope fractionation. It is noted that even the largest isotope effect may not cause fractionation if the reaction goes to completion, i.e., a quantitative reaction in which the reactant is completely transformed into the product. However, an isotopic fractionation will always be observed when a reaction has an isotope effect and the formation of the product is not quantitative (Hayes, 1982).

Equilibrium isotope fractionation

Isotope fractionation can occur in equilibrium, for example, between the various isotopic forms of carbon dioxide, bicarbonate, and carbonate ions (Zeebe and Wolf-Gladrow, 2001). As a rule: "The heavy isotope goes preferentially to the chemical compound in which the element is bound most strongly." (Bigeleisen, 1965). For example, in the temperature range between 0 and 25° C, the

$\delta^{13}C_{CO2}$ in seawater is 8–10‰ lower ("isotopically lighter") than $\delta^{13}C_{HCO3^-}$.

The fractionation factors for equilibrium fractionation involving three isotopes with masses $m_1 < m_2 < m_3$ usually scale such that $\alpha_{2/1} = \alpha_{3/1}^{\beta}$, where $\beta = (1/m_1 - 1/m_2)/(1/m_1 - 1/m_3)$ (Young et al., 2002). For the three stable oxygen isotopes: $^{17}\alpha = (^{18}\alpha)^{0.529}$.

Nonequilibrium ("kinetic") isotope fractionation

Nonequilibrium effects are associated with incomplete or unidirectional processes such as evaporation, kinetic isotope effects in chemical reactions, diffusion, or metabolic effects. Kinetic isotope effects in chemical reactions occur when reaction rates for compounds containing light or heavy isotopes are different, which is almost always the case and thus isotope fractionation can be expected. If the reservoir of reactants is finite, the isotope effect associated with the reaction will not only yield a product of different isotopic composition but will lead to a change in the isotopic composition of the reservoir as well (*Rayleigh distillation*; Bigeleisen and Wolfsberg, 1958). Kinetic isotope effects can quantitatively be understood on the basis of the 'transition state theory' (Bigeleisen and Wolfsberg, 1958). The fractionation factors for kinetic fractionation involving three isotopes with masses $m_1 < m_2 < m_3$ often scale such that $\alpha_{2/1} = \alpha_{3/1}^{\beta}$, where $\beta = \ln(m_1/m_2)/\ln(m_1/m_3)$ (Young et al., 2002). For the three stable oxygen isotopes: $^{17}\alpha = (^{18}\alpha)^{0.515}$.

"Mass-independent" fractionation

A mass-independent fractionation of stable oxygen isotopes was reported (for the first time) in 1973 in meteorites and in 1983 in laboratory studies (Thiemens and Heidenreich, 1983). These studies show differences in the isotopic compositions for certain compounds that contain ^{16}O only (Substance X) and Compounds X and compound Y with fractionation factors $^{17}\alpha$ and $^{18}\alpha$ (between X and Y) that are almost equal, i.e., $^{17}\alpha \approx {}^{18}\alpha$. These fractionation processes are called 'mass-independent'. They may occur at low pressures and, for example, play an essential role for stratospheric ozone. The resulting unusual composition of atmospheric oxygen has been used in the so-called 'triple-isotope method' to derive estimates of the biosphere productivity (Luz et al., 1999). A theoretical explanation based on an extension of the Rice, Ramsperger, Kassel, Marcus (RRKM) theory has been developed only recently (Gao and Marcus, 2001). A mass-independent isotope effect has also been observed during thermal decomposition of carbonates in vacuo (Miller et al., 2002).

Dieter A. Wolf-Gladrow and Richard E. Zeebe

Bibliography

Bigeleisen, J., 1965. Chemistry of isotopes. *Science*, **147**, 463–471.

Bigeleisen, J. and M.G. Mayer. Calculation of equilibrium constants for isotopic exchange reactions. J. Chem. Phus., 15: 261–267, 1947.

Bigeleisen, J., and Wolfsberg, M., 1958. Theoretical and experimental aspects of isotope effects in chemical kinetics. *Adv. Chem. Phys.*, **1**, 15–76.

Criss, R.E., 1999. *Principles of Stable Isotope Distribution.* New York: Oxford University Press, 264pp.

Gao, Y.Q., and Marcus, R.A., 2001. Strange and unconventional isotope effects in ozone formation. *Science*, **293**, 259–263.

Hayes, J.M., 1982. Fractionation et al.: An introduction to isotopic measurement and terminology. *Spectra*, **8**(4), 3–8.

Hoefs, J., 1997. *Stable Isotope Geochemistry*, (4th edn.). Heidelberg: Springer.

Luz, B., et al., 1999. Triple-isotope composition of atmospheric oxygen as a tracer of biosphere productivity. *Nature*, **400**, 547–550.

Miller, et al., 2002. Mass-independent fractionation of oxygen isotopes during thermal decomposition of carbonates. *Proc. Natl. Acad. Sci.*, **99**(17), 10988–10993.

Thiemens, M.H., and Heidenreich, J.E. III., 1983. The mass-independent fractionation of oxygen: A novel isotope effect and its possible cosmochemical implications. *Science*, **219**, 1073–1075.

Urey, H.C., 1947. The thermodynamic properties of isotopic substances. *J. Chem. Soc.*, 562–581.

Young, et al., 2002. Kinetic and equilibrium mass-dependent isotope fractionation laws in nature and their geochemical and cosmochemical significance. *Goechim. Cosmochim. Acta*, **66**(6), 1095–1104.

Zeebe, R.E., and Wolf-Gladrow, D., 2001. *CO_2 in Seawater: Equilibrium, Kinetics, Isotopes.* Amsterdam: Elsevier.

Cross-references

Carbon Isotopes, Stable
Oxygen Isotopes
Paleotemperatures and Proxy Reconstructions
Stable Isotope Analysis
Strontium Isotopes
Sulfur Isotopes